HHS Public Access

Author manuscript

Dev Cell. Author manuscript; available in PMC 2019 January 08.

Published in final edited form as:

Dev Cell. 2018 January 08; 44(1): 56–72.e4. doi:10.1016/j.devcel.2017.12.014.

Budding yeast has a minimal endomembrane system

Kasey J. Day[1], **Jason C. Casler**[1], and **Benjamin S. Glick**[1,*]

[1]Department of Molecular Genetics and Cell Biology, University of Chicago, 920 East 58th St., Chicago, IL 60637 USA, Tel. 773-702-5315, Fax 773-702-3172

Abstract

The endomembrane system consists of the secretory and endocytic pathways, which communicate by transport to and from the *trans*-Golgi network (TGN). In mammalian cells, the endocytic pathway includes early, late, and recycling endosomes. In budding yeast, different types of endosomes have been described, but the organization of the endocytic pathway has been unclear. We performed a spatial and temporal analysis of yeast endosomal markers and endocytic cargoes. Our results indicate that the yeast TGN also serves as an early and recycling endosome. In addition, as previously described, yeast contains a late or prevacuolar endosome (PVE). Endocytic cargoes localize to the TGN shortly after internalization, and manipulations that perturb export from the TGN can slow the passage of endocytic cargoes to the PVE. Yeast apparently lacks a distinct early endosome. Thus, yeast has a simple endocytic pathway that may reflect the ancestral organization of the endomembrane system.

eTOC Blurb

Although mammalian endocytic pathway has early, late, and recycling endosomes, the *Saccharomyces cerevisiae* system is unresolved. Day et al. show that yeast only has two endosome types: the *trans*-Golgi network, functioning as both early and recycling endosome, and the long-lived prevacuolar endosome, possibly reflecting ancestral organization of the endomembrane system.

Introduction

Organelles of the endomembrane system are linked by branched and often bidirectional trafficking routes. One major set of trafficking routes is the endocytic pathway. Endocytic compartments carry out sorting, recycling, and degradative functions (Maxfield and McGraw, 2004; Scott et al., 2014). The second major set of trafficking routes is the secretory

*Corresponding Author and Lead Contact: bsglick@uchicago.edu.

Author Contributions

K.J.D. designed and performed the majority of the experiments, created the figures, and wrote the manuscript. J.C.C. contributed at an early stage of the project by developing methods, reagents, and strains. B.S.G. supervised the project and edited the manuscript.

Declaration of Interests

The authors declare no competing interests.

pathway. Proteins exported from the ER transit the Golgi apparatus to the TGN, where they are sorted for delivery to the plasma membrane, to endosomes, or directly to lysosomes/vacuoles (Gadila and Kim, 2016; Guo et al., 2014). Cargo molecules travel either by being incorporated into transport vesicles or by remaining within a compartment as it matures. Each endomembrane compartment is distinguished by a unique group of molecular markers that include Rab GTPases, cargo adaptors, vesicle coats, vesicle tethers, fusogenic SNARE proteins, and specific lipids (Cai et al., 2007; Zerial and McBride, 2001).

In mammalian cells, endocytosed material appears first in an early endosome, also known as a sorting endosome (Maxfield and McGraw, 2004). Some components are then recycled to the plasma membrane via recycling endosomes, also known as the endosomal recycling compartment. The remainder of an early endosome matures into a late endosome, also known as a multivesicular body (MVB), which delivers its contents to a lysosome for degradation (Huotari and Helenius, 2011; Rink et al., 2005). Maturation of mammalian endosomes is driven by Rab conversion, in which the early endosome marker Rab5 is replaced by the late endosome marker Rab7 (Scott et al., 2014).

Mammalian endosomes exchange material with the TGN, which is the main site of communication between the secretory and endocytic pathways (De Matteis and Luini, 2008). The TGN is often in close proximity to recycling endosomes (Misaki et al., 2007), and exchange between these compartments is bidirectional: some toxins and receptors reach the TGN via recycling endosomes (Lin et al., 2004; Matsudaira et al., 2015), while some secretory proteins travel from the TGN to recycling endosomes en route to the cell surface (Ang et al., 2004; Lock and Stow, 2005; Thuenauer et al., 2014). Similarly, exchange between the TGN and late endosomes is bidirectional: receptors carrying lysosomal hydrolases move from the TGN to late endosomes, and the empty receptors return to the TGN (Braulke and Bonifacino, 2009; Kornfeld and Mellman, 1989).

The budding yeast *Saccharomyces cerevisiae* is useful for studying endocytic vesicle formation (Goode et al., 2015), but yeast endosomes are incompletely characterized. Researchers have assumed that yeast contains early endosomes like those in mammalian cells, as well as late endosomes that deliver material to the lysosome-like vacuole (Pelham, 2002; Piper et al., 1995). Support for this view came from biochemical and imaging data indicating that endocytosed material destined for the vacuole passes through two distinct types of endosomes (Hicke et al., 1997; Prescianotto-Baschong and Riezman, 1998; Singer-Krüger et al., 1993). Moreover, some endocytosed components can be recycled, suggesting that yeast has a compartment analogous to a recycling endosome (Lewis et al., 2000; MacDonald and Piper, 2017; Wiederkehr et al., 2000). The best characterized type of yeast endosome is the prevacuolar compartment, which resembles a late endosome and is often next to the vacuole (Adell et al., 2017; Hicke et al., 1997; Prescianotto-Baschong and Riezman, 1998). We will refer to this compartment as the prevacuolar endosome (PVE). The putative early and recycling endosomes in yeast are less well described.

A yeast early endosome could be defined functionally as the compartment in which material appears shortly after endocytosis. Yeast endocytosis is often tracked by labeling the plasma membrane with the dye FM 4-64, which is internalized to punctate structures that have been

designated early endosomes (Huckaba et al., 2004; Vida and Emr, 1995). However, those results must be interpreted with caution because FM 4-64 is seen in the TGN following internalization (Lewis et al., 2000). We have shown that FM 4-64-labeled structures previously assumed to be early endosomes were actually identical to the TGN (Bhave et al., 2014).

A yeast early endosome could be defined molecularly by the presence of specific marker proteins. For example, the SNARE Tlg1 localizes to structures that were described as early endosomes based on the presence of internalized tracers (Lewis et al., 2000; Prescianotto-Baschong and Riezman, 2002). Yet Tlg1 colocalizes at least partially with TGN markers (Lewis et al., 2000; McDonold and Fromme, 2014; Valdivia et al., 2002). Similarly, the processing protease Kex2 had been assumed to cycle between endosomes and the TGN, but our recent work revealed that Kex2 actually cycles from older to younger versions of the maturing TGN (Papanikou et al., 2015). Thus, an early endosome marker that does not also label the TGN has been elusive. Many yeast researchers acknowledge this ambiguity by referring to the "TGN/early endosome." Despite this nomenclature, the prevailing notion has been that yeast contains a distinct early endosome, which presumably matures into a PVE while exchanging material with the TGN (Arlt et al., 2015; Becuwe and Léon, 2014; Spang, 2015).

An additional question is whether yeast has recycling endosomes. A fraction of the internalized FM 4-64 recycles to the plasma membrane (Wiederkehr et al., 2000), and the SNARE Snc1 cycles through an intracellular compartment (Lewis et al., 2000). The Ypt31/32 GTPase pair and its effector Rcy1 have been implicated in recycling of Snc1 (Chen et al., 2005), but again, these proteins colocalize to a significant degree with TGN/early endosome markers (Chen et al., 2005; Jedd et al., 1997). Thus, there has been no compelling evidence for a distinct recycling endosome in yeast.

We propose that the yeast TGN also serves as an early and recycling endosome. This simple model explains many observations from the prior literature, and it is supported by the results described below. The implication is that budding yeast has a remarkably streamlined endomembrane system.

Results

S. cerevisiae has two types of endosomes

The starting assumption was that *S. cerevisiae* might contain early endosomes or recycling endosomes or both. To identify molecules that would label such compartments, we examined multiple protein and lipid species. Because candidate early and recycling endosome markers might localize at least partially to the TGN and/or PVE, we compared the localization of each candidate marker to two reference markers. The reference marker for the TGN was Sec7, a guanine nucleotide exchange factor (GEF) for Arf1 (Casanova, 2007; Losev et al., 2006). The reference marker for the PVE was Vps8, a subunit of the CORVET tethering complex (Arlt et al., 2015). Each candidate endosome marker was tagged with GFP and visualized together with either Sec7-mCherry or Vps8-mCherry. Tagging was done

by gene replacement except in the case of Rcy1, Snc1, and Ypt52, which were expressed as GFP-tagged second copies.

We captured two-color images by confocal microscopy and measured the percent of the punctate candidate marker signal that overlapped with each reference marker. Initial controls were proteins that should localize to the TGN. Arf1 is recruited to the TGN by Sec7, and the two proteins showed strong colocalization (Figure S1). (Some Arf1 is also expected to be present at the early Golgi (Peyroche et al., 2001), but that pool of tagged Arf1 was relatively small.) Pik1 is a phosphatidylinositol 4-kinase that generates PI(4)P at the TGN (Hama et al., 1999; Walch-Solimena and Novick, 1999), and Pik1 as well as a GFP-tagged PH domain that binds PI(4)P colocalized strongly with the TGN reference marker (Figure S1) (Daboussi et al., 2012; Levine and Munro, 2001). Similarly, clathrin as well as the AP-1 and Gga clathrin adaptors are present at the TGN (Daboussi et al., 2012; Dell'Angelica et al., 2000; Myers and Payne, 2013), and the clathrin heavy chain Chc1 and the AP-1 subunit Apl2 and Gga2 all colocalized with the TGN reference marker (Figure S1). With our assay, typical colocalization values for proteins presumed to be at the same compartment were in the range of 60–85%.

Candidates for markers of yeast early endosomes include the SNAREs Tlg1 and Tlg2. Tlg1 was reported to colocalize with labeled endocytic tracers (Prescianotto-Baschong and Riezman, 2002), and functional and microscopy studies implicated Tlg2 in endocytosis (Abeliovich et al., 1998; Séron et al., 1998). Yet both Tlg1 and Tlg2 showed substantial colocalization with the TGN reference marker (Figures 1 and S1).

Other markers could potentially label either early endosomes or the PVE or both. Mammalian early endosomes are defined by the presence of Rab5 (Zerial and McBride, 2001), and growing yeast cells express the Rab5 homologs Vps21 and Ypt52 (Nickerson et al., 2012; Singer-Krüger et al., 1994). However, we found that Vps21 and Ypt52 colocalized almost perfectly with the PVE reference marker (Figures 1 and S1). We also examined (a) Hse1, a subunit of the ESCRT-0 complex that initiates the formation of intraluminal vesicles in an MVB (Bilodeau et al., 2002; Henne et al., 2011); (b) Vps17, a subunit of the retromer complex that mediates retrograde traffic from endosomes to the TGN (Burd and Cullen, 2014; Seaman et al., 1998); (c) Snx4, a sorting nexin involved in a second endosome-to-TGN trafficking pathway (Hettema et al., 2003; Shi et al., 2011); and (d) the phosphoinositide PI(3)P, which was labeled using the FYVE domain of the mammalian early endosome marker EEA1 (Burd and Emr, 1998). Although mammalian versions of these markers are found at varying stages of the endosomal maturation pathway, Hse1, Vps17, and PI(3)P showed greater than 70% colocalization with the PVE reference marker (Figures 1 and S1). The overlap between Snx4 and the PVE reference marker Vps8 was somewhat lower because of a slight difference in shape between the two fluorescence patterns, perhaps due to the presence of Snx4 on endosomal tubules (Ma et al., 2017). Vps16, which is present in the CORVET complex with Vps8 and also in the HOPS tethering complex that acts at the vacuole (Angers and Merz, 2009; Peplowska et al., 2007), was found on the vacuolar membrane and in puncta that colocalized entirely with the PVE reference marker (Figure S1). An earlier paper presented evidence for slight differences in the timing of appearance of various markers at the PVE (Arlt et al., 2015), but our data do

not support this interpretation. Instead, markers that would label either an early or a late endosome in mammalian cells all label the PVE in yeast.

Next, we examined markers that could potentially label a recycling endosome. The Rab GTPase Ypt31 is a yeast homolog of mammalian Rab11, which localizes to recycling endosomes (Benli et al., 1996). But Ypt31 and its close relative Ypt32 have been identified as key regulators of exit from the TGN (Jedd et al., 1997), and in agreement with previous work, we observed Ypt31 primarily at the TGN (Figure 1) (Kim et al., 2016; McDonold and Fromme, 2014). An effector of Ypt31/32 is the F-box protein Rcy1, which functions in endocytic recycling (Chen et al., 2005; Wiederkehr et al., 2000), and we found that overexpressed Rcy1 colocalized with the TGN reference marker (Figure S1). Other potential recycling endosome markers are proteins that cycle between the plasma membrane and endocytic compartments. One such protein is the chitin synthase Chs3, which localizes to the plasma membrane or to intracellular compartments in a cell cycle-dependent manner (Santos and Snyder, 1997; Ziman et al., 1996). We found that intracellular Chs3 colocalized with the TGN reference marker (Figure 1), in agreement with previous reports (Zanolari et al., 2011). Another recycling protein is the SNARE Snc1, which is found at both the plasma membrane and endocytic compartments (Gurunathan et al., 2000; Lewis et al., 2000). With overexpressed Snc1, weak Snc1 signals could sometimes be detected at the PVE (arrowheads in Figure S1A), presumably because Snc1 cycles between the TGN and the PVE (Ma et al., 2017), but the brighter intracellular puncta corresponded to the TGN (Figure S1). Similarly, the Snc1 L96V mutant accumulates in intracellular puncta that were proposed to be recycling endosomes (Lewis et al., 2000), but this Snc1 mutant colocalized with Sec7 at the TGN (Figure S1). We infer that the yeast TGN mediates endocytic recycling.

In sum, for every candidate early or recycling endosome marker that we examined, the majority of the signal colocalized with the reference marker for either the TGN or the PVE. The only exceptions were AP-3 adaptor subunits, which were found near the TGN (see below), and Vps10, a vacuolar hydrolase receptor that cycles between the TGN and PVE and localizes about equally to both compartments (Figure S1C) (Cooper and Stevens, 1996; Papanikou et al., 2015). For yeast, neither we nor others have identified markers that might uniquely label early or recycling endosomes.

Proteins vary in their spatiotemporal patterns of association with the TGN

In many cases, a candidate endosome marker did not completely colocalize with the TGN or PVE reference marker, raising the possibility that some components have a second localization to distinct early or recycling endosomes. But alternative explanations can be envisioned. For example, with the TGN, incomplete colocalization could reflect the dynamics of maturing Golgi compartments—if the arrival and departure of a candidate marker are not synchronized with the arrival and departure of the TGN reference marker, the maturing TGN will sometimes label with only one or the other marker instead of both (Figure 2A). We have documented this effect for Kex2, which arrives and departs slightly before Sec7 during Golgi maturation (Papanikou et al., 2015). Thus, a full analysis of the relationship between two TGN markers requires live cell imaging.

This issue is illustrated by Tlg1. In static images, only ~50% of the Tlg1 signal overlaps with the Sec7 signal (Figure 1), and some structures label with Tlg1 but not with Sec7 (arrow in Figure 1A). Such structures were thought to represent early endosomes (Lewis et al., 2000; Xu et al., 2017). We revisited this question by comparing the dynamics of Tlg1 and Sec7 in 4D confocal movies. Tlg1 is not abundant, so we tagged it with HaloTag and labeled the fusion protein with the bright and photostable far-red ligand JF_{646} (Grimm et al., 2015) in cells expressing Sec7-GFP. Tlg1 consistently arrived at the TGN ~10–20 s before Sec7 and departed ~20–30 s before Sec7 (Figure 2B and Movie S1A). In a 5-min movie, a total of 32 structures that labeled with Tlg1 but not Sec7 could be followed unambiguously for at least 10 s, and each structure could be traced forward to a time point when it also contained Sec7 (Movie S2A).

The same type of analysis was performed with AP-1. Video microscopy showed previously that AP-1 is found at the TGN, where its levels peak after those of Sec7 (Daboussi et al., 2012). A somewhat different picture came from functional studies, which implicated AP-1 in the retrograde traffic of TGN proteins, leading to the idea that AP-1 acts at an endosome to recycle proteins to the TGN (Liu et al., 2008; Spang, 2015; Valdivia et al., 2002). In our static images, the AP-1 subunit Apl2 colocalized with Sec7 ~60% of the time (Figure S1), and some Apl2-labeled structures lacked Sec7 (arrow in Figure S1A). In movies of cells labeled with Apl2-GFP and Sec7-mCherry, Apl2 consistently arrived at the TGN ~20–40 s after Sec7 and departed ~10–15 s after Sec7 (Figure 2C and Movie S1B). In a 5-min movie, a total of 27 structures that labeled with Apl2 but not Sec7 could be followed unambiguously for at least 10 s, and each structure could be traced back to a time point when it also contained Sec7 (Movie S2B). The implication is that both Tlg1 and AP-1 are found exclusively at the TGN, where Tlg1 arrives earlier than the TGN reference marker Sec7 while AP-1 persists somewhat longer than Sec7.

A different and unique result was seen with the AP-3 adaptor, which helps to transport certain proteins directly from the TGN to the vacuole (Cowles et al., 1997; Llinares et al., 2015) and may also play a role in yeast endocytic trafficking (Toshima et al., 2014). We examined AP-3 localization using the Apl5 and Apl6 subunits. As a control, those two subunits colocalized completely with each other (Figure 2D). The AP-3 subunits were often in close proximity to Sec7-labeled TGN compartments (Figure 2D) (Angers and Merz, 2009). However, true colocalization with Sec7 was much lower for the AP-3 subunits than for most TGN markers. To clarify the relationship between AP-3 and the TGN, we made 4D confocal movies. AP-3 proved to be highly dynamic, with the movies showing many labeled structures that changed rapidly (Movie S3A). We simplified the analysis by deleting *ARF1* to generate fewer, larger TGN cisternae that exhibited nearly normal maturation dynamics (Bhave et al., 2014). In *arf1Δ* cells, most of the AP-3 remained close to TGN compartments, and preceded Sec7 in its arrival and departure times (Figure 2E and Movie S3B). In *ARF1* wild-type cells, even though AP-3 could not be easily tracked for the lifetime of a TGN compartment, the same physical and temporal relationships between AP-3 and Sec7 were apparent (Movie S3A). These results indicate that AP-3 associates with the maturing TGN.

The AP-3-containing structures are unusual because they are distinct from the nearby Sec7-labeled compartments in both location and shape (Figure 2D,E and Movie S3). One

possibility is that AP-3 defines a TGN domain that lacks Sec7. To test this idea, we internalized FM 4–64 under conditions that label the TGN (Bhave et al., 2014), with the assumption that this bulk membrane dye should partition into all connected membrane domains. Internalized FM 4–64 colocalized very well with Sec7, but poorly with AP-3 (Figure 2F). These results suggest that AP-3 marks either a non-membranous structure that is attached to the TGN, or a membranous compartment that is near the TGN but not always connected to it by a phospholipid bilayer. In either case, AP-3 can be placed in the category of TGN-associated markers.

The PVE is a long-lived compartment

If yeast cells lack early endosomes, where does the PVE come from? Our results argue against the existence of a mammalian-type endosomal maturation pathway in yeast. To gain insight into the origin and fate of PVE compartments, we performed 4D confocal microscopy of cells expressing Vps8-GFP. Most of the PVE compartments could be followed for the entire duration of a 15-min movie (Figure 3B and Movie S4). PVE compartments did not disappear, as might have been expected if they fused with vacuoles. For comparison, the same cells expressed Sec7-mCherry to label the TGN. The TGN structures showed the behavior previously described for this maturing compartment (Losev et al., 2006; Matsuura-Tokita et al., 2006), with the Sec7-mCherry signal persisting for ~70–90 s (Figure 3A and Movie S4). We also examined cells in which the PVE was labeled with both Vps8-mCherry and a second PVE marker, either GFP-FYVE or GFP-Vps21 (Movie S5). Those markers colocalized extensively with Vps8 and remained on Vps8-labeled PVE structures continuously. The implication is that PVE compartments are long-lived.

PVE compartments occasionally undergo fusion and fission (Arlt et al., 2015; Chi et al., 2014). These phenomena cause stepwise increases and decreases in the intensity of the Vps8-GFP signal, as illustrated by the blue trace in Figure 3B. Although some of the apparent fusion and fission events seen by fluorescence microscopy might reflect reversible clustering of PVE compartments (Adell et al., 2017), most PVE compartments in wild-type cells are not clustered (Nickerson et al., 2012), suggesting that we mainly observed true fusion and fission. The rates of fusion and fission were similar, with an average of 4.8 fusion events and 4.6 fission events per cell over the course of a 15-min movie (Figure 3C). Thus, a plausible mechanism for maintaining the number of PVE compartments per cell is a balance between fusion and fission.

The TGN is an early destination for bulk endocytosis

Because FM 4-64 is seen in the yeast TGN soon after endocytosis (Figure 2F) (Bhave et al., 2014), our working hypothesis was that the yeast TGN serves as an early endosome. This hypothesis predicted that internalized FM 4-64 should appear first in the TGN and then in the PVE. As a test, we generated a wave of labeled endocytic traffic by applying a 30 s pulse of FM 4-64, followed by a chase with SCAS, which quenched dye that had not been internalized (Bhave et al., 2014). The cells expressed Sec7-CFP and Vps8-YFP so that FM 4-64 could be visualized simultaneously with TGN and PVE compartments. FM 4-64 labels both the recycling and degradative branches of the endocytic pathway, with a portion of the dye molecules returning to the cell surface while the remainder ultimately reach the vacuole

(Vida and Emr, 1995; Wiederkehr et al., 2000). To visualize the compartments involved, we captured static images at periodic intervals during the chase period, and then counted the number of TGN and PVE structures that contained detectable levels of FM 4-64 at each time point. FM 4-64 labeling of the TGN peaked at around 3 min after internalization (Figure 4A,B). Loss of FM 4-64 from the TGN was gradual despite the rapid turnover of this compartment, presumably because dye-containing membrane recycled from older to younger TGN cisternae. FM 4-64 labeling of the PVE peaked at around 10 min after internalization, then gradually decreased as the dye began to appear in the vacuolar membrane (Figure 4A,B). These kinetics fit with the idea that after endocytosis, the TGN is the first destination of bulk membrane, followed by the PVE and vacuole.

To test whether endocytic traffic necessarily passes through the TGN, we used a *pik1-83* mutant strain, which expresses a thermosensitive version of the Pik1 kinase that generates PI(4)P at the TGN (Audhya et al., 2000; Hendricks et al., 1999). Reduction of PI(4)P levels compromises export from the TGN (Walch-Solimena and Novick, 1999). In *pik1-83* cells at the permissive temperature of 22°C, traff ic of internalized FM 4-64 to the TGN, PVE, and vacuole were essentially normal (Figure 4C,D). By contrast, in *pik1-83* cells at the nonpermissive temperature of 37°C, FM 4-64 rapidly reached the TGN and then persisted there, probably due to a combination of reduced transport to the PVE and slowed recycling to the plasma membrane (Figure 4C,D). An isogenic wild-type *PIK1* strain showed no defect in FM 4-64 traffic at 37°C (Figure S2). These results match earlier reports (Audhya et al., 2000; Walch-Solimena and Novick, 1999), except that the TGN is now identified as the site of FM 4-64 accumulation in *pik1* mutant cells. Thus, most or all of the internalized membrane labeled by FM 4-64 evidently passes through the TGN.

The TGN is an early destination for signal-dependent endocytosis

Although FM 4-64 is useful for tracking initial steps of endocytosis, the internalized dye travels to multiple destinations. A simpler route is followed by the mating pheromone α-factor, which binds to the Ste2 receptor at the cell surface and then travels unidirectionally to the vacuole for degradation (Arlt et al., 2015; Toshima et al., 2006). The signal for endocytosis and vacuolar degradation is ubiquitination of Ste2 (Hicke and Riezman, 1996). To visualize this signal-dependent endocytic traffic, we incubated Cy5-labeled α-factor with yeast cells on ice for 2 h, then shifted the cells to room temperature to trigger a wave of internalization (Arlt et al., 2015; Toshima et al., 2006). The long preincubation on ice dramatically accelerated internalization of α-factor (Figure 5A), presumably because it generated endocytic vesicle intermediates that were poised for immediate endocytosis. Internalized α-factor accumulated in the PVE (Figure 5B,C) as previously reported (Arlt et al., 2015). However, at the earliest time points, dim but clearly visible α-factor signals were also detected in TGN compartments (Figure 5B,C). By 5 min after the temperature shift, the internalized α-factor had chased entirely to the PVE, where it remained until gradually appearing in the vacuole beginning at ~18 min (Figure 5B,C). The early appearance of α-factor in the TGN is consistent with the possibility that Ste2-bound α-factor travels first to the TGN after endocytosis.

According to this hypothesis, after reaching the TGN, Ste2-bound α-factor is rapidly sorted into carriers and transported to the PVE. A candidate for such a sorting system at the TGN is the Gga adaptors, which recognize proteins destined for the PVE (Costaguta et al., 2001; Scott et al., 2004). We tested whether deletion of the *GGA1* and *GGA2* genes would slow export of internalized α-factor from the TGN. Indeed, in a *gga1Δ gga2Δ* strain, internalized α-factor remained visible in a subset of the TGN compartments for tens of minutes (Figure 5D,E). Turnover of TGN compartments labeled by Sec7-GFP occurred with similar kinetics in *gga1*Δ *gga2*Δ cells as in wild-type cells (data not shown) (Daboussi et al., 2012), suggesting that α-factor was retained by recycling within the maturing TGN. Compared to wild-type cells, the *gga1Δ gga2Δ* cells showed somewhat reduced accumulation of α-factor in the PVE and negligible appearance of α-factor in the vacuole (Figure 5D,E). The time to reach half-maximum labeling of the PVE with α-factor was less than 1 min in wild-type cells versus nearly 4 min in *gga1*Δ *gga2*Δ cells (Figure 5C,E). Loss of the Gga adaptors likely has multiple effects—e.g., intraluminal vesicle formation at the PVE may be compromised, thereby blocking delivery to the vacuole (Deng et al., 2009; Lauwers et al., 2009). With this caveat, the results support the interpretation that Ste2-bound α-factor travels first to the TGN and then exits to the PVE in a process that involves the Gga adaptors.

Another yeast plasma membrane protein that undergoes signal-dependent endocytosis is the methionine permease Mup1 (Menant et al., 2006). Upon addition of methionine to the media, Mup1 is ubiquitinated and internalized, then delivered to the vacuole for degradation (Lin et al., 2008). At 5 min after methionine addition to wild-type cells, internalized Mup1 was seen in the PVE (Figure S3A), where it remained visible for at least 20 min (Figure S3A,C) (Prosser et al., 2010). Very little Mup1 was detected in the TGN, with only an occasional TGN compartment having a detectable signal after methionine addition (Figure S3C). In a *gga1Δ gga2Δ* strain, at 3–5 min after methionine addition, internalized Mup1 was almost never visible in the PVE, but was sometimes visible in TGN compartments (Figure S3B). Although the percentage of *gga1Δ gga2Δ* cells displaying internalized Mup1 was low at those early time points, the kinetic data were consistent with initial appearance in the TGN followed by delivery to the PVE (Figure S3C). Mup1 remained visible in the TGN of *gga1Δ gga2Δ* cells for at least 20 min while also progressively appearing in the PVE (Figure S3B,C). We postulate that like Ste2-bound α-factor, Mup1 passed rapidly through the TGN in a Gga-dependent manner. However, sequential appearance in the TGN and PVE was harder to detect for Mup1 than for α-factor because internalization of Mup1 was less well synchronized.

In a separate attempt to trap internalized α-factor at the TGN, we deleted the SNARE Pep12 to accumulate endocytic intermediates upstream of the PVE (Gerrard et al., 2000). Compared to wild-type cells, *pep12*Δ cells exhibited more heterogeneity in the structures that labeled with α-factor, but we were able to measure colocalization with the TGN and PVE markers. In *pep12*Δ cells, internalized α-factor appeared at the TGN within a few minutes and persisted there, while appearance at the PVE was strongly delayed (Figure 5F,G). The combined results with α-factor and Mup1 provide evidence that signal-dependent endocytic traffic in yeast involves passage through the TGN en route to the PVE.

Yeast endocytic vesicles fuse with the TGN

The simplest interpretation of our data is that endocytic vesicles are targeted directly to the TGN and not to the PVE. To test this hypothesis directly, we imaged endocytic vesicles containing FM 4-64 (Huckaba et al., 2004) in cells that also expressed a GFP-tagged marker for the PVE or TGN. For the PVE, the marker was Vps8-GFP. For the TGN, the choice of marker was trickier because we found that internalized FM 4-64 appeared in TGN structures ~10 s earlier than Sec7 (Figure S4A and Movie S6). Thus, if Sec7-GFP were used to label the TGN, an endocytic vesicle might fuse with a TGN compartment that was not yet labeled. We therefore used Kex2-GFP, which arrives at the TGN 5–20 s earlier than Sec7 (Papanikou et al., 2015). Another challenge was to limit the number of endocytic vesicles containing FM 4-64 so that individual vesicles could be tracked. A typical yeast cell has ~30 endocytic structures that persist for ~30 s (Carlsson et al., 2002; Lu and Drubin, 2017), so approximately one endocytic vesicle forms per second. Using a custom flow chamber (Barrero et al., 2016), we exposed yeast cells to a 5 s pulse of FM 4-64 followed by a chase with SCAS to quench external dye, thereby generating about five labeled endocytic vesicles per cell. A control experiment (Figure S4B) confirmed that FM 4-64 failed to be internalized in cells pretreated with latrunculin A, an actin polymerization inhibitor that blocks endocytosis (Weinberg and Drubin, 2012). The fate of the endocytic vesicles was then followed by 4D confocal microscopy.

Endocytic vesicles containing FM 4-64 were frequently seen to approach and merge with TGN compartments marked with Kex2-GFP. The FM 4-64 and GFP signals could then be tracked together for multiple movie frames and often persisted for about a minute after the merge event, suggesting that the compartments that received endocytic vesicles were at an early stage of TGN maturation (Movie S7A). Figures 6 and S4C show representative fusions of endocytic vesicles with TGN compartments. In movies of 33 cells, we observed merge events for 66% of the FM 4-64 puncta (145 out of 219) within 2 min of internalization. Although structures containing FM 4-64 occasionally approached PVE compartments (Movie S7B and Figure S4D), in movies of 37 cells, we observed no merge events with the PVE for the 175 FM 4-64 puncta that could be tracked. These results confirm that the first destination in the yeast endocytic pathway is the TGN.

Discussion

Early endosomes are well characterized in mammalian cells (Figure 7A) and have long been thought to exist in yeast (Hicke et al., 1997; Pelham, 2002; Singer-Krüger et al., 1993; Séron et al., 1998), yet we present evidence that *S. cerevisiae* lacks distinct early endosomes. This point is illustrated most compellingly by 4D movies of FM 4-64-labeled endocytic vesicles fusing with the TGN. Previous studies have shown that both FM 4-64 and α-factor are internalized at actin patches into vesicles marked with the actin-binding protein Abp1, suggesting that these cargoes are transported in the same type of endocytic vesicles (Huckaba et al., 2004; Toshima et al., 2006; Weinberg and Drubin, 2012). Thus, the yeast TGN evidently functions as the first destination for both bulk endocytosis and signal-dependent endocytosis, in a pathway that has no parallel in mammalian cells.

Why has the role of the TGN in yeast endocytic traffic previously been obscure? Three factors have contributed. First, yeast researchers studying the secretory and endocytic pathways have assumed that they were looking at different organelles. For example, an elegant study visualized the fusion of endocytic vesicles with “endosomal sorting compartments”, which had been labeled by incubating cells with FM 4-64 and then imaging 7 min later (Huckaba et al., 2004). We find that at 7 min after FM 4-64 internalization, most of the labeled puncta are TGN compartments, suggesting that those authors were seeing fusion of endocytic vesicles with the TGN. Another example came from our analysis of effects of the *arf1Δ* mutation, which reportedly caused enlargement of Golgi cisternae and also of endocytic compartments labeled with FM 4-64 (Gaynor et al., 1998). It turned out that those endocytic compartments were identical to the TGN (Bhave et al., 2014). Thus, when endocytic markers were examined but TGN markers were not, the yeast TGN was described as an endosome.

A second factor that has obscured the role of the TGN in yeast endocytic traffic is that unlike FM 4-64, proteins with endocytic signals can apparently pass quickly through the TGN. We obtained evidence for this phenomenon with Ste2-bound α-factor. That cargo follows a ubiquitination-dependent route through endosomes to the vacuole, and it had not previously been detected at the TGN (Arlt et al., 2015; Toshima et al., 2014). We now document that a transient pool of α-factor can be seen at the TGN. Definitive proof that this transient pool reflects obligatory passage of α-factor through the TGN would require a complete and reversible block of TGN export. Unfortunately, no such protocol is currently available. For example, while a *pik1* mutation increases the persistence of FM 4-64 in the TGN, this mutation has no visible effect on α-factor trafficking (unpublished data), likely because Pik1 exerts its PI 4-kinase activity at the TGN after the Gga adaptors have already transported proteins to the PVE (Costaguta et al., 2001; Scott et al., 2004). On the other hand, when we delete the Gga adaptors, a substantial and persistent pool of Ste2-bound α-factor is seen at the TGN, presumably because passage to the PVE is slowed. Deletion of the SNARE Pep12 prevents fusion of transport carriers with the PVE and traps α-factor at the TGN even more strongly, presumably because the *pep12*Δ mutation disrupts recycling between the PVE and TGN, thereby depleting components needed to export α-factor from the TGN. Another yeast protein that undergoes signal-dependent endocytosis is the methionine permease Mup1 (Menant et al., 2006). Although the analysis is more challenging than for Ste2-bound α-factor, we find that deletion of the Gga adaptors increases the levels of internalized Mup1 at the TGN. Similarly, the monocarboxylate transporter Jen1 reportedly passed through the TGN on its way to the vacuole, and Jen1 accumulated in the TGN in a strain lacking the Gga adaptors (Becuwe and Léon, 2014). That study concluded that Jen1 is internalized to a maturing early endosome and then travels to the TGN and back to the PVE, but a simpler interpretation is that Jen1 is internalized directly to the TGN before reaching the PVE. The available data suggest that the initial destination for various types of yeast endocytic cargo is the TGN.

A third factor that has obscured the role of the TGN in yeast endocytic traffic is subtler. In static images, TGN proteins often colocalize only partially with one another, leading to the idea that some proteins have a dual localization to the TGN and early endosomes. But the TGN is a maturing compartment (Losev et al., 2006; Matsuura-Tokita et al., 2006), so a

given TGN structure will possess different markers over time (Papanikou et al., 2015). Here we document this phenomenon with the SNARE Tlg1 and the AP-1 clathrin adaptor, which had been implicated in recycling from endosomes but actually seem to reside exclusively at the TGN, where Tlg1 arrives and departs before Sec7 while AP-1 arrives and departs after Sec7. We conclude that when characterizing a component of the TGN, a full localization analysis requires kinetic data from live cell microscopy.

In addition to early endosomes, mammalian cells contain recycling endosomes (Figure 7A), so we asked whether yeast cells contain distinct recycling endosomes. Possible markers for recycling endosomes in yeast include (a) the Ypt31/32 GTPases, which are homologs of the mammalian recycling endosome marker Rab11 (Chen et al., 2005), (b) wild-type and some mutant versions of the SNARE Snc1, which cycles between the plasma membrane and intracellular compartments (Lewis et al., 2000), and (c) Rcy1, a Ypt31/32 effector implicated in Snc1 recycling (Chen et al., 2005; Wiederkehr et al., 2000). We find that Ypt31, Snc1, and Rcy1 all localize to the TGN. Another possible marker is the chitin synthase Chs3, which cycles between the plasma membrane and intracellular “chitosomes” (Bartnicki-Garcia, 2006; Flores Martinez and Schwencke, 1988; Ziman et al., 1996). However, we see Chs3 at the TGN, and others have also concluded that chitosomes are identical to the TGN (Spang, 2015; Zanolari et al., 2011). Finally, bulk membrane recycling in the yeast endocytic pathway was previously observed using FM 4-64 (Wiederkehr et al., 2000), and our localization data suggest that this recycling step occurs at the TGN. The combined results imply that the yeast TGN is an endocytic recycling compartment. Thus, we can depict yeast as having a minimal endomembrane system, with the TGN playing a central role as a sorting station for both secretory and endocytic cargoes (Figure 7B).

This model raises a question about the biogenesis of PVE compartments. In mammalian cells, early endosomes mature into late endosomes, which fuse with lysosomes to deliver their contents (Bright et al., 2005; Luzio et al., 2007). By contrast, we find that PVE compartments persist for a long time and perhaps indefinitely. The only dynamic behaviors that we have observed for PVE compartments are fission and homotypic fusion. It therefore seems likely that the PVE proliferates by fission, which is presumably slightly more frequent than homotypic fusion over the course of an average cell cycle.

Our perspective on the yeast endocytic pathway sheds light on earlier observations. For example, inactivation of the TGN-localized Pik1 was reported to inhibit transport of internalized FM 4-64 to the vacuole (Audhya et al., 2000; Walch-Solimena and Novick, 1999), and deletion of the TGN-localized Gga adaptors was reported to inhibit transport of internalized plasma membrane proteins to the vacuole (Becuwe and Léon, 2014; Scott et al., 2004). Those effects could be indirect, but now that we have identified the TGN as the first station in the yeast endocytic pathway, a more likely interpretation is that PI(4)P and the Gga adaptors have direct roles in the traffic of internalized material from the TGN. Additionally, yeast endocytic vesicles have been reported to move along actin tracks (Huckaba et al., 2004; Toshima et al., 2006), and yeast TGN compartments are associated with the actin cytoskeleton (Arai et al., 2008; Rossanese et al., 2001), providing a mechanism for efficient delivery of endocytic vesicles to the TGN. Finally, even though yeast has homologs of proteins implicated in the maturation of mammalian endosomes (Huotari and Helenius,

2011; Nordmann et al., 2010), yeast endosomes have not been seen to mature (Arlt et al., 2015), a result that can now be understood by viewing the PVE as a stable compartment.

The absence of a distinct early endosome in yeast has implications for understanding the role of AP-1. When AP-1 was first identified in mammalian cells, it was assumed to act in the forward traffic of proteins from the TGN to endosomes (Hinners and Tooze, 2003), but then the Gga adaptors were shown to mediate TGN-to-endosome traffic (Black and Pelham, 2000; Dell'Angelica et al., 2000). Meanwhile, yeast AP-1 was implicated in retrograde traffic (Liu et al., 2008; Spang, 2015; Valdivia et al., 2002), a function that is probably conserved in mammalian cells (Bonifacino, 2014; Hinners and Tooze, 2003; Matsudaira et al., 2015). Yeast AP-1 is important for maintaining the TGN localization of proteins such as Chs3 and Tlg1 (Spang, 2015; Valdivia et al., 2002). The favored hypothesis has been that AP-1 mediates recycling of TGN proteins from early endosomes to the TGN. Alternatively, it has been noted that AP-1 could mediate recycling from maturing TGN compartments (Liu et al., 2008; Valdivia et al., 2002), and our recent work favors this interpretation (Papanikou et al., 2015). Now we present evidence that yeast AP-1 resides exclusively at the TGN, strongly suggesting that AP-1 mediates intra-Golgi recycling. This idea can explain why the TGN has different types of clathrin adaptors: Gga adaptors for transport to the late endosome/PVE, and AP-1 for retrieval from older to younger TGN cisternae (Papanikou et al., 2015).

The AP-3 adaptor is more mysterious. AP-3 functions, perhaps independently of clathrin, to deliver certain proteins from the yeast TGN directly to the vacuole (Cowles et al., 1997; Llinares et al., 2015) or from the mammalian early or recycling endosome directly to the lysosome (Peden et al., 2004; Zlatic et al., 2013). Yeast AP-3 has also been implicated in endocytosis (Toshima et al., 2014), an observation possibly related to our finding that endocytic traffic passes through the TGN. Surprisingly, we find that the physical association of yeast AP-3 with the TGN is less tight than for most TGN markers. The majority of yeast AP-3 apparently resides not on the TGN surface, but rather in unidentified structures that are somehow tethered to the TGN. The nature of this structure merits further investigation. However, we suspect that the results will not alter our view of the TGN as the nexus of the yeast secretory and endocytic pathways.

The discussion so far has emphasized differences between the endomembrane systems of yeast and mammals, but there are also fundamental similarities. It is useful to highlight the relationships of the yeast TGN and PVE compartments to the different types of mammalian endosomes (Figure 7).

We propose that the yeast TGN combines properties of the mammalian TGN and recycling endosomes. Interestingly, in mammalian cells, the TGN and recycling endosome are closely related—the recycling endosome is often near the TGN, and the two compartments share molecular markers such as Sec7 family proteins, PI(4)P, and AP-1 (Grant and Donaldson, 2009; Matsudaira et al., 2015). Moreover, some secretory cargoes pass through the mammalian recycling endosome, which can therefore be considered a post-TGN compartment of the secretory pathway (Ang et al., 2004; Lock and Stow, 2005; Thuenauer et al., 2014). It seems that yeast assigns secretory and endocytic recycling functions to the

TGN, whereas mammalian cells partially segregate those functions between the TGN and recycling endosomes. The yeast TGN is capable of sorting material to either the plasma membrane or the PVE, and this capability is harnessed by both the secretory and endocytic pathways, making the TGN the central sorting station in the cell.

We further propose that the yeast PVE combines properties of the mammalian early and late endosomes. In agreement with earlier reports (Arlt et al., 2015; Ma et al., 2017), yeast components that might have been expected to mark separate endosome populations actually colocalize extensively at the PVE. For example, even though Rab5 is a marker for mammalian early endosomes, we see the yeast Rab5 homologs Vps21 and Ypt52 at the PVE. The mammalian late endosome is marked by Rab7, but in yeast, the homologous Ypt7 protein is found on the vacuole (Cabrera et al., 2009). Those results are hard to reconcile with an endosomal maturation pathway of the type that operates in mammalian cells (Huotari and Helenius, 2011; Rink et al., 2005). According to that paradigm, the PVE should be a transient structure that forms by maturation and ultimately merges with the vacuole. Instead, our 4D microscopy data indicate that PVE compartments are long-lived and maintain a stable composition. We speculate that PVE compartments undergo “kiss-and-run” events with the vacuole, thereby delivering intraluminal vesicles to the vacuole for degradation. This idea seems reasonable given that mammalian late endosomes can undergo “kiss-and-run” events with lysosomes (Bright et al., 2005). In this scenario, compared to yeast, mammalian cells do two things differently: they deliver endocytic vesicles to dedicated early endosomes instead of the TGN, and they continually regenerate endosomes through maturation and turnover.

In yeast, a prior analysis of vacuolar protein sorting (*vps*) mutants suggested that some secretory proteins pass through endosomes en route to the cell surface (Harsay and Schekman, 2002). However, it seems unlikely that a secretory protein would travel to the PVE and then to the plasma membrane. The earlier results might have been due to indirect effects of the *vps* mutants. According to this view, normal vacuolar protein sorting is needed for the TGN to segregate cargo proteins into different types of secretory vesicles. Further insight will require a better understanding of sorting mechanisms at the TGN (Kienzle and von Blume, 2014).

The yeast endocytic pathway shows a striking similarity to that of plant cells, in which the TGN is also the first destination of endocytic traffic (Dettmer et al., 2006; Viotti et al., 2010). Based on this comparison, it is possible that the ancestral endomembrane system resembled that of yeast. The membrane traffic circuit shown in Figure 7B is sufficient to carry out the basic functions of the secretory and endocytic pathways, namely, sorting of biosynthetic and endocytic cargoes to either the plasma membrane or the endosome/lysosome/vacuole. According to this hypothesis, mammalian cell evolution increased the complexity of the endocytic pathway through two innovations. First, the endocytic recycling functions of the TGN were transferred to the recycling endosome, which is a derivative of the TGN. Second, endocytic vesicles were redirected from the TGN to endosomes, and the ancestral functions of a stable endosome were divided between early and late endosomes that turn over through maturation. Theoretical studies suggested that such maturation pathways evolve readily (Mani and Thattai, 2016). Alternatively, both plants and budding

yeast may have independently lost features of the endomembrane system that were present in the eukaryotic ancestor. For instance, the early endosome-specific Rab4 was lost during the evolution of budding yeasts and plants (Field et al., 2007). A broader functional analysis of different eukaryotes should help to distinguish between conserved and organism-specific aspects of the endocytic pathway.

STAR Methods

Contact for Reagent and Resource Sharing

Further information and requests for resources and reagents should be directed to and will be fulfilled by the Lead Contact, Benjamin S. Glick (bsglick@uchicago.edu).

Experimental Model and Subject Details

Yeast strains were derived from the haploid *S. cerevisiae* strain JK9-3da, with genotype *leu2-3,112 ura3-52 rme1 trp1 his4 HMLa* (Heitman et al., 1991). Yeast cells were grown in rich glucose medium (YPD), or in nonfluorescent minimal glucose dropout medium (NSD) (Bevis et al., 2002) in baffled flasks at room temperature.

The *ARF1* and *GGA2* genes were deleted by amplifying a kanMX cassette from pFA6-kanMX4 using primers with flanking regions corresponding to 40–42 bp upstream and downstream of the *ARF1* and *GGA2* ORFs (Wach et al., 1994). Yeast were transformed with the amplified fragment and selected for resistance to G418 (U.S. Biological, Salem, MA). The *GGA1* and *PEP12* genes were deleted by amplifying a hygromycin resistance cassette from pFA6-hphMX4 using primers with flanking regions corresponding to the 39–41 bp upstream and downstream of the *GGA2* and *PEP12* ORFs (Goldstein and McCusker, 1999). Yeast were transformed with the amplified fragment and selected for resistance to hygromycin B (Corning Life Sciences, Corning, NY).

Isogenic strains containing either the temperature-sensitive *pik1-83* or wild-type *PIK1* allele were provided by Jeremy Thorner, and the *ade2-101* allele was reverted to wild-type by transformation with a fragment corresponding to *ADE2*. GFP tags used for various constructs were 1x, 3x, or 6x msGFP (Fitzgerald and Glick, 2014) and iGFP, a variant of sGFP (Losev et al., 2006) with the L221K mutation and the msGFP termini. Six tandem copies of an mCherry variant called mCherry2B, which has modified N- and C-termini, was used as a C-terminal tag for Sec7, Vps8, and Apl5. Sec7 was tagged with six tandem copies of msCFP, which was generated by Ivy Fitzgerald from SCFP3A (Kremers et al., 2006) by introducing S30R, Y39N, N105T, Y145F, I171V, L231H, and the msGFP N- and C- termini. Vps8 was tagged with six tandem copies of iYFP, which is iGFP with T65G, V68L, S72A, T203Y. Tlg1 was N-terminally tagged with HaloTag (Promega, Madison, WI) using a yeast codon-optimized gene (GenScript, Piscataway, NJ). The iGFP-Ypt52 construct was expressed from its own promoter as an integrating second copy at the *TRP1* locus. Rcy1 and the PH domain of Osh1 were N-terminally tagged with iGFP, and the fusion genes subcloned between the *TPI1* promoter and *CYC1* terminator were integrated at the *TRP1* locus. pRS406-GFP-SNC1 was provided by Nava Segev, and was modified by site-directed mutagenesis to generate pRS406-GFP-SNC1(L96V) (Chen et al., 2011; Lewis et al., 2000).

pRS424-GFP-FYVE(EEA1) was provided by Chris Burd (Burd and Emr, 1998). All proteins other than Ypt52, Rcy1, Snc1, Osh1(PH), and FYVE(EEA1) were tagged by gene replacement using the pop-in/pop-out method to obtain expression at endogenous levels (Rossanese et al., 1999; Rothstein, 1991). Tagged constructs were confirmed as functional whenever possible, based on normal growth for essential genes as well as comparisons with previously reported fluorescence patterns and organelle dynamics. Plasmids generated in this study will be available from Addgene.

Method Details

Fluorescence microscopy—For fluorescence imaging, yeast cultures were grown in NSD, with amino acid dropouts when necessary, and imaged at room temperature. Static images were collected of live cells attached to a concanavalin A-coated coverglass-bottom dish containing NSD medium (Losev et al., 2006) on an SP5 or SP8 microscope (Leica, Buffalo Grove, IL) or an LSM 880 microscope (Zeiss, Thornwood, NY) equipped with a 1.4 NA/63x oil objective, using a 40–60 nm pixel size and a 0.25–0.30 μm Z-step interval and 20–30 optical sections. For quantifying FM 4-64FX (Life Technologies, Carlsbad, CA) localization in fixed *pik1-83* and isogenic *PIK1* cells, α-factor localization in *pep12*Δ cells, and Mup1 localization in live cells, the cells were compressed under a coverslip and center slices were collected by widefield microscopy on an Axioplan 2 epifluorescence microscope (Zeiss) equipped with a 1.4 NA/100x oil objective and a digital camera (Hamamatsu, Skokie, IL). For quantifying α-factor localization in WT and *gga1*Δ *gga2*Δ cells, fixed cells were compressed under a coverslip and imaged on an LSM 880 microscope using a 50 nm pixel size and 0.30 μm Z-step interval and ~10 optical sections. 4D confocal movies were collected on a Leica SP5 or SP8 microscope using an 80 nm pixel size and a 0.25–0.30 μm Z-step interval and 20–30 optical sections, with a Z-stack collected every 0.5–2.0 s.

Static images were converted to 16-bit and average projected, then range-adjusted to the minimum and maximum pixel values in ImageJ (http://rsbweb.nih.gov/ij/). To process movies, a Gaussian blur with radius 0.75 pixels was applied in ImageJ to fluorescence channels (Day et al., 2016), which were then deconvolved with Huygens Essential (Scientific Volume Imaging, Hilversum, The Netherlands) using the CMLE (Classical Maximum Likelihood Estimation) algorithm (Day et al., 2017), and then corrected for bleaching using an ImageJ plugin (cmci.embl.de/downloads/bleach_corrector). Movies were converted to hyperstacks and average projected, then range-adjusted to maximize contrast in ImageJ. Custom ImageJ plugins (Papanikou et al., 2015) were used to generate montages of time series, select individual structures and remove background structures, convert edited montages to hyperstacks, and measure fluorescence intensities.

HaloTag labeling—To visualize HaloTag-Tlg1, 5 μM JF_{646} ligand, provided by Luke Lavis (Grimm et al., 2015), was added to cells from a 5 mM stock in DMSO. Cells were incubated with shaking at room temperature for 30 min, washed twice and resuspended in NSD, then adhered to a concanavalin A-coated coverglass-bottom dish. Movies were captured immediately on a Leica SP5.

FM 4-64 labeling—For the FM 4-64 time course analysis, and for comparing the localization of internalized FM 4-64 with that of AP-3, live cells were adhered to a concanavalin A-coated coverglass-bottom dish containing NSD, then 0.8 μM FM 4-64 (Life Technologies) was added from a 1 mM stock in DMSO. After 30 s, 2.4 μM SCAS (4-sulfonato calix[8]arene, sodium salt; Biotium, Hayward, CA) was added from a 1 mM aqueous stock solution to quench extracellular dye. The cells were then imaged at the times indicated.

For *pik1-83* and isogenic *PIK1* cells, cultures were grown at 22°C, then split and either kept at 22°C or shifted to 37°C for 15 min b efore treatment with 0.8 μM FM 4-64FX for 30 s, followed by 2.4 μM SCAS. Cultures were kept at 22°C or 37°C and samples were fixed at intervals between 1 and 30 min after addition of FM 4-64FX by combining equal volumes of yeast culture with ice-cold fixative (100 mM potassium phosphate at pH 6.5, 2 mM $MgCl_2$, 8% formaldehyde, 0.5% glutaraldehyde) while vortexing. Cells were fixed on ice for 1 hour, then washed twice with ice-cold PBS at pH 7.5 and imaged.

For the latrunculin A control experiment, cells were either left untreated or incubated with 200 μM latrunculin A for 10 min at 22°C. Then 5 μM FM 4-64FX was added, followed after 5 s by 15 μM SCAS. Then 10 s later cells were fixed as described above, and imaged on a Leica SP5.

For tracking endocytic vesicles, cells were adhered to a concanavalin A-coated coverslip and placed in a flow chamber filled with NSD (Barrero et al., 2016). Fresh NSD containing 5 μM FM 4-64 was flowed in for a 5 s pulse, followed directly by a chase with NSD containing 15 μM SCAS. Movies were then captured immediately on a Leica SP8.

α-factor labeling—Cultures were placed on ice for 15 min, then mixed with 2 μM Cy5-α-factor (ordered from Sigma-Aldrich as a custom peptide with Cy5 conjugated to the lysine side chain) from a 1 mM stock in 0.1 M sodium acetate, pH 5.2. After 2 h on ice, cells were washed in ice-cold NSD, then resuspended in room temperature NSD to initiate α-factor internalization. Samples were fixed on ice as described above at intervals up to 40 min, then washed with PBS and imaged.

Mup1 endocytosis assay—Cells grown in NSD lacking methionine (NSD-Met) were adhered to a concanavalin A-coated coverglass-bottom dish containing NSD-Met, then 20 μg/ml of methionine was added. Cells were imaged at intervals between 3 and 20 min (Prosser et al., 2010) either on a confocal microscope, or on a widefield microscope for quantification.

Quantification and Statistical Analysis

Quantifying colocalization—For colocalization analysis, the fraction of the green candidate marker punctate signal that overlapped with the red reference marker punctate signal was quantified in ImageJ as follows (Levi et al., 2010; Papanikou et al., 2015). Fluorescence channels from average projected images were converted to grayscale, noise was removed using the Smooth function, and images were inverted to generate black signal on a white background. Binary masks were created using the DynamicThreshold 1d plugin

(www.gcsca.net/IJ/Dynamic.html) by taking the mean thresholded image with a mask size of 15–25 and a constant C value of 10–20 in order to detect punctate signal over varying background levels. The mask for the green channel was then subtracted from an inversion of its original grayscale image to result in an image of only the punctate green signal. The mask of the red signal was then subtracted from the image of the punctate green signal to create an image of the punctate green signal that overlapped with red signal. The mean values of the resulting image and the punctate green signal image were calculated using the Measure function, then the first was divided by the second to calculate the percentage overlap out of total punctate green signal. A modified version of this procedure was used to quantify the number of Sec7 or Vps8 structures that had detectable FM 4-64, α-factor, or Mup1 signal. Masks were created as described above for each of the three fluorescence channels. As an example, the FM 4-64 mask image was subtracted from the inverted Sec7 mask image to generate a binary image of the overlapping puncta. The number of FM 4-64 and Sec7 overlapping puncta that lacked Vps8 signal and were at least 40 nm^2 was counted using the Analyze Particles function in ImageJ, then divided by the total number of Sec7 puncta that lacked Vps8 signal, yielding the percentage of unambiguous Sec7 structures positive for FM 4-64. A similar method was used to count unambiguous Sec7 structures positive for α-factor or Mup1 as well as unambiguous Vps8 structures positive for FM 4-64, α-factor, and Mup1. Vacuole signal was calculated as the percentage of cells with FM 4-64 or α-factor visible in vacuolar structures. Vacuolar identity was confirmed using the vacuolar membrane marker Vph1-GFP. Internalized FM 4-64 or Cy5-α-factor localized to the membrane or interior, respectively, of Vph1-GFP-labeled vacuoles at 15–40 min after internalization (data not shown). Each colocalization value reported is the mean ± SEM for at least the number of cells listed in the figure legend.

Data and Software Availability

DNA sequences—DNA constructs were designed using SnapGene software (GSL Biotech, Chicago, IL). For the constructs used in this study, Supplementary File S1 contains annotated sequence files that can be opened with SnapGene Viewer (www.snapgene.com/products/snapgene_viewer).

Supplementary Material

Refer to Web version on PubMed Central for supplementary material.

Acknowledgments

This work was supported by NIH grant R01 GM104010. K.J.D. and J.C.C. were supported by NIH training grant T32 GM007183. Thanks for assistance with fluorescence microscopy to Vytas Bindokas and Christine Labno at the Integrated Microscopy Core Facility, which is supported by the NIH-funded Cancer Center Support Grant P30 CA014599. Additional thanks to Nava Segev for providing the Snc1 plasmid and helpful feedback, to Chris Burd for providing the GFP-FYVE construct, to Jeremy Thorner for providing *pik1-83* and *PIK1* strains, and to Luke Lavis for providing the JF_{646} dye.

References

Abeliovich H, Grote E, Novick P, Ferro-Novick S. Tlg2p, a yeast syntaxin homolog that resides on the Golgi and endocytic structures. J Biol Chem. 1998; 273:11719–11727. [PubMed: 9565594]

Adell MAY, Migliano SM, Upadhyayula S, Bykov YS, Sprenger S, Pakdel M, Vogel GF, Jih G, Skillern W, Behrouzi R, et al. Recruitment dynamics of ESCRT-III and Vps4 to endosomes and implications for reverse membrane budding. Elife. 2017; 6

Ang AL, Taguchi T, Francis S, Fölsch H, Murrells LJ, Pypaert M, Warren G, Mellman I. Recycling endosomes can serve as intermediates during transport from the Golgi to the plasma membrane of MDCK cells. J Cell Biol. 2004; 167:531–543. [PubMed: 15534004]

Angers CG, Merz AJ. HOPS interacts with Apl5 at the vacuole membrane and is required for consumption of AP-3 transport vesicles. Mol Biol Cell. 2009; 20:4563–4574. [PubMed: 19741093]

Arai S, Noda Y, Kainuma S, Wada I, Yoda K. Ypt11 functions in bud-directed transport of the Golgi by linking Myo2 to the coatomer subunit Ret2. Curr Biol. 2008; 18:987–991. [PubMed: 18595704]

Arlt H, Auffarth K, Kurre R, Lisse D, Piehler J, Ungermann C. Spatiotemporal dynamics of membrane remodeling and fusion proteins during endocytic transport. Mol Biol Cell. 2015; 26:1357–1370. [PubMed: 25657322]

Audhya A, Foti M, Emr SD. Distinct roles for the yeast phosphatidylinositol 4-kinases, Stt4p and Pik1p, in secretion, cell growth, and organelle membrane dynamics. Mol Biol Cell. 2000; 11:2673–2689. [PubMed: 10930462]

Bajaj A, Celić A, Ding FX, Naider F, Becker JM, Dumont ME. A fluorescent alpha-factor analogue exhibits multiple steps on binding to its G protein coupled receptor in yeast. Biochemistry. 2004; 43:13564–13578. [PubMed: 15491163]

Barrero JJ, Papanikou E, Casler JC, Day KJ, Glick BS. An improved reversibly dimerizing mutant of the FK506-binding protein FKBP. Cell Logist. 2016; 6:e1204848. [PubMed: 27738551]

Bartnicki-Garcia S. Chitosomes: past, present and future. FEMS Yeast Res. 2006; 6:957–965. [PubMed: 16981903]

Becuwe M, Léon S. Integrated control of transporter endocytosis and recycling by the arrestin-related protein Rod1 and the ubiquitin ligase Rsp5. Elife. 2014; 3:e03307.

Benli M, Döring F, Robinson DG, Yang X, Gallwitz D. Two GTPase isoforms, Ypt31p and Ypt32p, are essential for Golgi function in yeast. EMBO J. 1996; 15:6460–6475. [PubMed: 8978673]

Bevis BJ, Hammond AT, Reinke CA, Glick BS. De novo formation of transitional ER sites and Golgi structures in Pichia pastoris. Nat Cell Biol. 2002; 4:750–756. [PubMed: 12360285]

Bhave M, Papanikou E, Iyer P, Pandya K, Jain BK, Ganguly A, Sharma C, Pawar K, Austin J, Day KJ, et al. Golgi enlargement in Arf-depleted yeast cells is due to altered dynamics of cisternal maturation. J Cell Sci. 2014; 127:250–257. [PubMed: 24190882]

Bilodeau PS, Urbanowski JL, Winistorfer SC, Piper RC. The Vps27p Hse1p complex binds ubiquitin and mediates endosomal protein sorting. Nat Cell Biol. 2002; 4:534–539. [PubMed: 12055639]

Black MW, Pelham HR. A selective transport route from Golgi to late endosomes that requires the yeast GGA proteins. J Cell Biol. 2000; 151:587–600. [PubMed: 11062260]

Bonifacino JS. Adaptor proteins involved in polarized sorting. J Cell Biol. 2014; 204:7–17. [PubMed: 24395635]

Braulke T, Bonifacino JS. Sorting of lysosomal proteins. Biochim Biophys Acta. 2009; 1793:605–614. [PubMed: 19046998]

Bright NA, Gratian MJ, Luzio JP. Endocytic delivery to lysosomes mediated by concurrent fusion and kissing events in living cells. Curr Biol. 2005; 15:360–365. [PubMed: 15723798]

Burd C, Cullen PJ. Retromer: a master conductor of endosome sorting. Cold Spring Harb Perspect Biol. 2014; 6

Burd CG, Emr SD. Phosphatidylinositol(3)-phosphate signaling mediated by specific binding to RING FYVE domains. Mol Cell. 1998; 2:157–162. [PubMed: 9702203]

Cabrera M, Ostrowicz CW, Mari M, LaGrassa TJ, Reggiori F, Ungermann C. Vps41 phosphorylation and the Rab Ypt7 control the targeting of the HOPS complex to endosome-vacuole fusion sites. Mol Biol Cell. 2009; 20:1937–1948. [PubMed: 19193765]

Cai H, Reinisch K, Ferro-Novick S. Coats, tethers, Rabs, and SNAREs work together to mediate the intracellular destination of a transport vesicle. Dev Cell. 2007; 12:671–682. [PubMed: 17488620]

Carlsson AE, Shah AD, Elking D, Karpova TS, Cooper JA. Quantitative analysis of actin patch movement in yeast. Biophys J. 2002; 82:2333–2343. [PubMed: 11964224]

Casanova JE. Regulation of Arf activation: the Sec7 family of guanine nucleotide exchange factors. Traffic. 2007; 8:1476–1485. [PubMed: 17850229]

Chen SH, Chen S, Tokarev AA, Liu F, Jedd G, Segev N. Ypt31/32 GTPases and their novel F-box effector protein Rcy1 regulate protein recycling. Mol Biol Cell. 2005; 16:178–192. [PubMed: 15537705]

Chen SH, Shah AH, Segev N. Ypt31/32 GTPases and their F-Box effector Rcy1 regulate ubiquitination of recycling proteins. Cell Logist. 2011; 1:21–31. [PubMed: 21686101]

Chi RJ, Liu J, West M, Wang J, Odorizzi G, Burd CG. Fission of SNX-BAR-coated endosomal retrograde transport carriers is promoted by the dynamin-related protein Vps1. J Cell Biol. 2014; 204:793–806. [PubMed: 24567361]

Cooper AA, Stevens TH. Vps10p cycles between the late-Golgi and prevacuolar compartments in its function as the sorting receptor for multiple yeast vacuolar hydrolases. J Cell Biol. 1996; 133:529–541. [PubMed: 8636229]

Costaguta G, Stefan CJ, Bensen ES, Emr SD, Payne GS. Yeast Gga coat proteins function with clathrin in Golgi to endosome transport. Mol Biol Cell. 2001; 12:1885–1896. [PubMed: 11408593]

Cowles CR, Odorizzi G, Payne GS, Emr SD. The AP-3 adaptor complex is essential for cargo-selective transport to the yeast vacuole. Cell. 1997; 91:109–118. [PubMed: 9335339]

Daboussi L, Costaguta G, Payne GS. Phosphoinositide-mediated clathrin adaptor progression at the trans-Golgi network. Nat Cell Biol. 2012; 14:239–248. [PubMed: 22344030]

Day KJ, La Rivière PJ, Chandler T, Bindokas VP, Ferrier NJ, Glick BS. Improved deconvolution of very weak confocal signals. F1000Res. 2017; 6:787. [PubMed: 28868135]

Day KJ, Papanikou E, Glick BS. 4D Confocal Imaging of Yeast Organelles. Methods Mol Biol. 2016; 1496:1–11. [PubMed: 27631997]

De Matteis MA, Luini A. Exiting the Golgi complex. Nat Rev Mol Cell Biol. 2008; 9:273–284. [PubMed: 18354421]

Dell'Angelica EC, Puertollano R, Mullins C, Aguilar RC, Vargas JD, Hartnell LM, Bonifacino JS. GGAs: a family of ADP ribosylation factor-binding proteins related to adaptors and associated with the Golgi complex. J Cell Biol. 2000; 149:81–94. [PubMed: 10747089]

Deng Y, Guo Y, Watson H, Au WC, Shakoury-Elizeh M, Basrai MA, Bonifacino JS, Philpott CC. Gga2 mediates sequential ubiquitin-independent and ubiquitin-dependent steps in the trafficking of ARN1 from the trans-Golgi network to the vacuole. J Biol Chem. 2009; 284:23830–23841. [PubMed: 19574226]

Dettmer J, Hong-Hermesdorf A, Stierhof YD, Schumacher K. Vacuolar H+-ATPase activity is required for endocytic and secretory trafficking in Arabidopsis. Plant Cell. 2006; 18:715–730. [PubMed: 16461582]

Field MC, Gabernet-Castello C, Dacks JB. Reconstructing the evolution of the endocytic system: insights from genomics and molecular cell biology. Adv Exp Med Biol. 2007; 607:84–96. [PubMed: 17977461]

Fitzgerald I, Glick BS. Secretion of a foreign protein from budding yeasts is enhanced by cotranslational translocation and by suppression of vacuolar targeting. Microb Cell Fact. 2014; 13:125. [PubMed: 25164324]

Flores Martinez A, Schwencke J. Chitin synthetase activity is bound to chitosomes and to the plasma membrane in protoplasts of Saccharomyces cerevisiae. Biochim Biophys Acta. 1988; 946:328–336. [PubMed: 2974729]

Gadila SKG, Kim K. Cargo trafficking from the trans-Golgi network towards the endosome. Biol Cell. 2016; 108:205. [PubMed: 27061938]

Gaynor EC, Chen CY, Emr SD, Graham TR. ARF is required for maintenance of yeast Golgi and endosome structure and function. Mol Biol Cell. 1998; 9:653–670. [PubMed: 9487133]

Gerrard SR, Levi BP, Stevens TH. Pep12p is a multifunctional yeast syntaxin that controls entry of biosynthetic, endocytic and retrograde traffic into the prevacuolar compartment. Traffic. 2000; 1:259–269. [PubMed: 11208109]

Goldstein AL, McCusker JH. Three new dominant drug resistance cassettes for gene disruption in Saccharomyces cerevisiae. Yeast. 1999; 15:1541–1553. [PubMed: 10514571]

Goode BL, Eskin JA, Wendland B. Actin and endocytosis in budding yeast. Genetics. 2015; 199:315–358. [PubMed: 25657349]

Grant BD, Donaldson JG. Pathways and mechanisms of endocytic recycling. Nat Rev Mol Cell Biol. 2009; 10:597–608. [PubMed: 19696797]

Grimm JB, English BP, Chen J, Slaughter JP, Zhang Z, Revyakin A, Patel R, Macklin JJ, Normanno D, Singer RH, et al. A general method to improve fluorophores for live-cell and single-molecule microscopy. Nat Methods. 2015; 12:244–250. [PubMed: 25599551]

Guo Y, Sirkis DW, Schekman R. Protein sorting at the trans-Golgi network. Annu Rev Cell Dev Biol. 2014; 30:169–206. [PubMed: 25150009]

Gurunathan S, Chapman-Shimshoni D, Trajkovic S, Gerst JE. Yeast exocytic v-SNAREs confer endocytosis. Mol Biol Cell. 2000; 11:3629–3643. [PubMed: 11029060]

Hama H, Schnieders EA, Thorner J, Takemoto JY, DeWald DB. Direct involvement of phosphatidylinositol 4-phosphate in secretion in the yeast Saccharomyces cerevisiae. J Biol Chem. 1999; 274:34294–34300. [PubMed: 10567405]

Harsay E, Schekman R. A subset of yeast vacuolar protein sorting mutants is blocked in one branch of the exocytic pathway. J Cell Biol. 2002; 156:271–285. [PubMed: 11807092]

Heitman J, Movva NR, Hiestand PC, Hall MN. FK 506-binding protein proline rotamase is a target for the immunosuppressive agent FK 506 in Saccharomyces cerevisiae. Proc Natl Acad Sci U S A. 1991; 88:1948–1952. [PubMed: 1705713]

Hendricks KB, Wang BQ, Schnieders EA, Thorner J. Yeast homologue of neuronal frequenin is a regulator of phosphatidylinositol-4-OH kinase. Nat Cell Biol. 1999; 1:234–241. [PubMed: 10559922]

Henne WM, Buchkovich NJ, Emr SD. The ESCRT pathway. Dev Cell. 2011; 21:77–91. [PubMed: 21763610]

Hettema EH, Lewis MJ, Black MW, Pelham HR. Retromer and the sorting nexins Snx4/41/42 mediate distinct retrieval pathways from yeast endosomes. EMBO J. 2003; 22:548–557. [PubMed: 12554655]

Hicke L, Riezman H. Ubiquitination of a yeast plasma membrane receptor signals its ligand-stimulated endocytosis. Cell. 1996; 84:277–287. [PubMed: 8565073]

Hicke L, Zanolari B, Pypaert M, Rohrer J, Riezman H. Transport through the yeast endocytic pathway occurs through morphologically distinct compartments and requires an active secretory pathway and Sec18p/N-ethylmaleimide-sensitive fusion protein. Mol Biol Cell. 1997; 8:13–31. [PubMed: 9017592]

Hinners I, Tooze SA. Changing directions: clathrin-mediated transport between the Golgi and endosomes. J Cell Sci. 2003; 116:763–771. [PubMed: 12571274]

Huckaba TM, Gay AC, Pantalena LF, Yang HC, Pon LA. Live cell imaging of the assembly, disassembly, and actin cable-dependent movement of endosomes and actin patches in the budding yeast, Saccharomyces cerevisiae. J Cell Biol. 2004; 167:519–530. [PubMed: 15534003]

Huotari J, Helenius A. Endosome maturation. EMBO J. 2011; 30:3481–3500. [PubMed: 21878991]

Jedd G, Mulholland J, Segev N. Two new Ypt GTPases are required for exit from the yeast trans-Golgi compartment. J Cell Biol. 1997; 137:563–580. [PubMed: 9151665]

Kienzle C, von Blume J. Secretory cargo sorting at the trans-Golgi network. Trends Cell Biol. 2014; 24:584–593. [PubMed: 24841758]

Kim JJ, Lipatova Z, Majumdar U, Segev N. Regulation of Golgi Cisternal Progression by Ypt/Rab GTPases. Dev Cell. 2016; 36:440–452. [PubMed: 26906739]

Kornfeld S, Mellman I. The biogenesis of lysosomes. Annu Rev Cell Biol. 1989; 5:483–525. [PubMed: 2557062]

Kremers GJ, Goedhart J, van Munster EB, Gadella TW. Cyan and yellow super fluorescent proteins with improved brightness, protein folding, and FRET Förster radius. Biochemistry. 2006; 45:6570–6580. [PubMed: 16716067]

Lauwers E, Jacob C, André B. K63-linked ubiquitin chains as a specific signal for protein sorting into the multivesicular body pathway. J Cell Biol. 2009; 185:493–502. [PubMed: 19398763]

Levi SK, Bhattacharyya D, Strack RL, Austin JR, Glick BS. The yeast GRASP Grh1 colocalizes with COPII and is dispensable for organizing the secretory pathway. Traffic. 2010; 11:1168–1179. [PubMed: 20573068]

Levine TP, Munro S. Dual targeting of Osh1p, a yeast homologue of oxysterol-binding protein, to both the Golgi and the nucleus-vacuole junction. Mol Biol Cell. 2001; 12:1633–1644. [PubMed: 11408574]

Lewis MJ, Nichols BJ, Prescianotto-Baschong C, Riezman H, Pelham HR. Specific retrieval of the exocytic SNARE Snc1p from early yeast endosomes. Mol Biol Cell. 2000; 11:23–38. [PubMed: 10637288]

Lin CH, MacGurn JA, Chu T, Stefan CJ, Emr SD. Arrestin-related ubiquitin-ligase adaptors regulate endocytosis and protein turnover at the cell surface. Cell. 2008; 135:714–725. [PubMed: 18976803]

Lin SX, Mallet WG, Huang AY, Maxfield FR. Endocytosed cation-independent mannose 6-phosphate receptor traffics via the endocytic recycling compartment en route to the trans-Golgi network and a subpopulation of late endosomes. Mol Biol Cell. 2004; 15:721–733. [PubMed: 14595110]

Liu K, Surendhran K, Nothwehr SF, Graham TR. P4-ATPase requirement for AP-1/clathrin function in protein transport from the trans-Golgi network and early endosomes. Mol Biol Cell. 2008; 19:3526–3535. [PubMed: 18508916]

Llinares E, Barry AO, André B. The AP-3 adaptor complex mediates sorting of yeast and mammalian PQ-loop-family basic amino acid transporters to the vacuolar/lysosomal membrane. Sci Rep. 2015; 5:16665. [PubMed: 26577948]

Lock JG, Stow JL. Rab11 in recycling endosomes regulates the sorting and basolateral transport of E-cadherin. Mol Biol Cell. 2005; 16:1744–1755. [PubMed: 15689490]

Losev E, Reinke CA, Jellen J, Strongin DE, Bevis BJ, Glick BS. Golgi maturation visualized in living yeast. Nature. 2006; 441:1002–1006. [PubMed: 16699524]

Lu R, Drubin DG. Selection and stabilization of endocytic sites by Ede1, a yeast functional homologue of human Eps15. Mol Biol Cell. 2017; 28:567–575. [PubMed: 28057762]

Luzio JP, Pryor PR, Bright NA. Lysosomes: fusion and function. Nat Rev Mol Cell Biol. 2007; 8:622–632. [PubMed: 17637737]

Ma M, Burd CG, Chi RJ. Distinct complexes of yeast Snx4 family SNX-BARs mediate retrograde trafficking of Snc1 and Atg27. Traffic. 2017; 18:134–144. [PubMed: 28026081]

MacDonald C, Piper RC. Genetic dissection of early endosomal recycling highlights a TORC1-independent role for Rag GTPases. J Cell Biol. 2017; 216:3275–3290. [PubMed: 28768685]

Mani S, Thattai M. Stacking the odds for Golgi cisternal maturation. Elife. 2016; 5:e16231. [PubMed: 27542195]

Matsudaira T, Niki T, Taguchi T, Arai H. Transport of the cholera toxin B-subunit from recycling endosomes to the Golgi requires clathrin and AP-1. J Cell Sci. 2015; 128:3131–3142. [PubMed: 26136365]

Matsuura-Tokita K, Takeuchi M, Ichihara A, Mikuriya K, Nakano A. Live imaging of yeast Golgi cisternal maturation. Nature. 2006; 441:1007–1010. [PubMed: 16699523]

Maxfield FR, McGraw TE. Endocytic recycling. Nat Rev Mol Cell Biol. 2004; 5:121–132. [PubMed: 15040445]

McDonold CM, Fromme JC. Four GTPases differentially regulate the Sec7 Arf-GEF to direct traffic at the trans-golgi network. Dev Cell. 2014; 30:759–767. [PubMed: 25220393]

Menant A, Barbey R, Thomas D. Substrate-mediated remodeling of methionine transport by multiple ubiquitin-dependent mechanisms in yeast cells. EMBO J. 2006; 25:4436–4447. [PubMed: 16977312]

Misaki R, Nakagawa T, Fukuda M, Taniguchi N, Taguchi T. Spatial segregation of degradation- and recycling-trafficking pathways in COS-1 cells. Biochem Biophys Res Commun. 2007; 360:580–585. [PubMed: 17606221]

Myers MD, Payne GS. Clathrin, adaptors and disease: insights from the yeast Saccharomyces cerevisiae. Front Biosci (Landmark Ed). 2013; 18:862–891. [PubMed: 23747853]

Nickerson DP, Russell MR, Lo SY, Chapin HC, Milnes JM, Merz AJ. Termination of isoform-selective Vps21/Rab5 signaling at endolysosomal organelles by Msb3/Gyp3. Traffic. 2012; 13:1411–1428. [PubMed: 22748138]

Nordmann M, Cabrera M, Perz A, Bröcker C, Ostrowicz C, Engelbrecht-Vandré S, Ungermann C. The Mon1-Ccz1 complex is the GEF of the late endosomal Rab7 homolog Ypt7. Curr Biol. 2010; 20:1654–1659. [PubMed: 20797862]

Papanikou E, Day KJ, Austin J, Glick BS. COPI selectively drives maturation of the early Golgi. Elife. 2015; 4:e13232. [PubMed: 26709839]

Peden AA, Oorschot V, Hesser BA, Austin CD, Scheller RH, Klumperman J. Localization of the AP-3 adaptor complex defines a novel endosomal exit site for lysosomal membrane proteins. J Cell Biol. 2004; 164:1065–1076. [PubMed: 15051738]

Pelham HR. Insights from yeast endosomes. Curr Opin Cell Biol. 2002; 14:454–462. [PubMed: 12383796]

Peplowska K, Markgraf DF, Ostrowicz CW, Bange G, Ungermann C. The CORVET tethering complex interacts with the yeast Rab5 homolog Vps21 and is involved in endo-lysosomal biogenesis. Dev Cell. 2007; 12:739–750. [PubMed: 17488625]

Peyroche A, Courbeyrette R, Rambourg A, Jackson CL. The ARF exchange factors Gea1p and Gea2p regulate Golgi structure and function in yeast. J Cell Sci. 2001; 114:2241–2253. [PubMed: 11493664]

Piper RC, Cooper AA, Yang H, Stevens TH. VPS27 controls vacuolar and endocytic traffic through a prevacuolar compartment in Saccharomyces cerevisiae. J Cell Biol. 1995; 131:603–617. [PubMed: 7593183]

Prescianotto-Baschong C, Riezman H. Morphology of the yeast endocytic pathway. Mol Biol Cell. 1998; 9:173–189. [PubMed: 9436999]

Prescianotto-Baschong C, Riezman H. Ordering of compartments in the yeast endocytic pathway. Traffic. 2002; 3:37–49. [PubMed: 11872141]

Prosser DC, Whitworth K, Wendland B. Quantitative analysis of endocytosis with cytoplasmic pHluorin chimeras. Traffic. 2010; 11:1141–1150. [PubMed: 20626707]

Rink J, Ghigo E, Kalaidzidis Y, Zerial M. Rab conversion as a mechanism of progression from early to late endosomes. Cell. 2005; 122:735–749. [PubMed: 16143105]

Rossanese OW, Reinke CA, Bevis BJ, Hammond AT, Sears IB, O'Connor J, Glick BS. A role for actin, Cdc1p, and Myo2p in the inheritance of late Golgi elements in Saccharomyces cerevisiae. J Cell Biol. 2001; 153:47–62. [PubMed: 11285273]

Rossanese OW, Soderholm J, Bevis BJ, Sears IB, O'Connor J, Williamson EK, Glick BS. Golgi structure correlates with transitional endoplasmic reticulum organization in Pichia pastoris and Saccharomyces cerevisiae. J Cell Biol. 1999; 145:69–81. [PubMed: 10189369]

Rothstein R. Targeting, disruption, replacement, and allele rescue: integrative DNA transformation in yeast. Methods Enzymol. 1991; 194:281–301. [PubMed: 2005793]

Santos B, Snyder M. Targeting of chitin synthase 3 to polarized growth sites in yeast requires Chs5p and Myo2p. J Cell Biol. 1997; 136:95–110. [PubMed: 9008706]

Scott CC, Vacca F, Gruenberg J. Endosome maturation, transport and functions. Semin Cell Dev Biol. 2014; 31:2–10. [PubMed: 24709024]

Scott PM, Bilodeau PS, Zhdankina O, Winistorfer SC, Hauglund MJ, Allaman MM, Kearney WR, Robertson AD, Boman AL, Piper RC. GGA proteins bind ubiquitin to facilitate sorting at the trans-Golgi network. Nat Cell Biol. 2004; 6:252–259. [PubMed: 15039776]

Seaman MN, McCaffery JM, Emr SD. A membrane coat complex essential for endosome-to-Golgi retrograde transport in yeast. J Cell Biol. 1998; 142:665–681. [PubMed: 9700157]

Shi Y, Stefan CJ, Rue SM, Teis D, Emr SD. Two novel WD40 domain-containing proteins, Ere1 and Ere2, function in the retromer-mediated endosomal recycling pathway. Mol Biol Cell. 2011; 22:4093–4107. [PubMed: 21880895]

Singer-Krüger B, Frank R, Crausaz F, Riezman H. Partial purification and characterization of early and late endosomes from yeast. Identification of four novel proteins. J Biol Chem. 1993; 268:14376–14386. [PubMed: 8314797]

Singer-Krüger B, Stenmark H, Düsterhöft A, Philippsen P, Yoo JS, Gallwitz D, Zerial M. Role of three rab5-like GTPases, Ypt51p, Ypt52p, and Ypt53p, in the endocytic and vacuolar protein sorting pathways of yeast. J Cell Biol. 1994; 125:283–298. [PubMed: 8163546]

Spang A. The Road not Taken: Less Traveled Roads from the TGN to the Plasma Membrane. Membranes (Basel). 2015; 5:84–98. [PubMed: 25764365]

Séron K, Tieaho V, Prescianotto-Baschong C, Aust T, Blondel MO, Guillaud P, Devilliers G, Rossanese OW, Glick BS, Riezman H, et al. A yeast t-SNARE involved in endocytosis. Mol Biol Cell. 1998; 9:2873–2889. [PubMed: 9763449]

Thuenauer R, Hsu YC, Carvajal-Gonzalez JM, Deborde S, Chuang JZ, Römer W, Sonnleitner A, Rodriguez-Boulan E, Sung CH. Four-dimensional live imaging of apical biosynthetic trafficking reveals a post-Golgi sorting role of apical endosomal intermediates. Proc Natl Acad Sci U S A. 2014; 111:4127–4132. [PubMed: 24591614]

Toshima JY, Nishinoaki S, Sato Y, Yamamoto W, Furukawa D, Siekhaus DE, Sawaguchi A, Toshima J. Bifurcation of the endocytic pathway into Rab5-dependent and -independent transport to the vacuole. Nat Commun. 2014; 5:3498. [PubMed: 24667230]

Toshima JY, Toshima J, Kaksonen M, Martin AC, King DS, Drubin DG. Spatial dynamics of receptor-mediated endocytic trafficking in budding yeast revealed by using fluorescent alpha-factor derivatives. Proc Natl Acad Sci U S A. 2006; 103:5793–5798. [PubMed: 16574772]

Valdivia RH, Baggott D, Chuang JS, Schekman RW. The yeast clathrin adaptor protein complex 1 is required for the efficient retention of a subset of late Golgi membrane proteins. Dev Cell. 2002; 2:283–294. [PubMed: 11879634]

Vida TA, Emr SD. A new vital stain for visualizing vacuolar membrane dynamics and endocytosis in yeast. J Cell Biol. 1995; 128:779–792. [PubMed: 7533169]

Viotti C, Bubeck J, Stierhof YD, Krebs M, Langhans M, van den Berg W, van Dongen W, Richter S, Geldner N, Takano J, et al. Endocytic and secretory traffic in Arabidopsis merge in the trans-Golgi network/early endosome, an independent and highly dynamic organelle. Plant Cell. 2010; 22:1344–1357. [PubMed: 20435907]

Wach A, Brachat A, Pöhlmann R, Philippsen P. New heterologous modules for classical or PCR-based gene disruptions in Saccharomyces cerevisiae. Yeast. 1994; 10:1793–1808. [PubMed: 7747518]

Walch-Solimena C, Novick P. The yeast phosphatidylinositol-4-OH kinase pik1 regulates secretion at the Golgi. Nat Cell Biol. 1999; 1:523–525. [PubMed: 10587649]

Weinberg J, Drubin DG. Clathrin-mediated endocytosis in budding yeast. Trends Cell Biol. 2012; 22:1–13. [PubMed: 22018597]

Wiederkehr A, Avaro S, Prescianotto-Baschong C, Haguenauer-Tsapis R, Riezman H. The F-box protein Rcy1p is involved in endocytic membrane traffic and recycling out of an early endosome in Saccharomyces cerevisiae. J Cell Biol. 2000; 149:397–410. [PubMed: 10769031]

Xu P, Hankins HM, MacDonald C, Erlinger SJ, Frazier MN, Diab NS, Piper RC, Jackson LP, MacGurn JA, Graham TR. COPI mediates recycling of an exocytic SNARE by recognition of a ubiquitin sorting signal. Elife. 2017; 6

Zanolari B, Rockenbauch U, Trautwein M, Clay L, Barral Y, Spang A. Transport to the plasma membrane is regulated differently early and late in the cell cycle in Saccharomyces cerevisiae. J Cell Sci. 2011; 124:1055–1066. [PubMed: 21363887]

Zerial M, McBride H. Rab proteins as membrane organizers. Nat Rev Mol Cell Biol. 2001; 2:107–117. [PubMed: 11252952]

Ziman M, Chuang JS, Schekman RW. Chs1p and Chs3p, two proteins involved in chitin synthesis, populate a compartment of the Saccharomyces cerevisiae endocytic pathway. Mol Biol Cell. 1996; 7:1909–1919. [PubMed: 8970154]

Zlatic SA, Grossniklaus EJ, Ryder PV, Salazar G, Mattheyses AL, Peden AA, Faundez V. Chemical-genetic disruption of clathrin function spares adaptor complex 3-dependent endosome vesicle biogenesis. Mol Biol Cell. 2013; 24:2378–2388. [PubMed: 23761069]

Highlights

- The budding yeast *Saccharomyces cerevisiae* lacks a distinct early endosome
- The yeast *trans*-Golgi network is the first destination for endocytic traffic
- The yeast *trans*-Golgi network also acts as a recycling endosome
- The yeast prevacuolar endosome is a non-maturing stable compartment

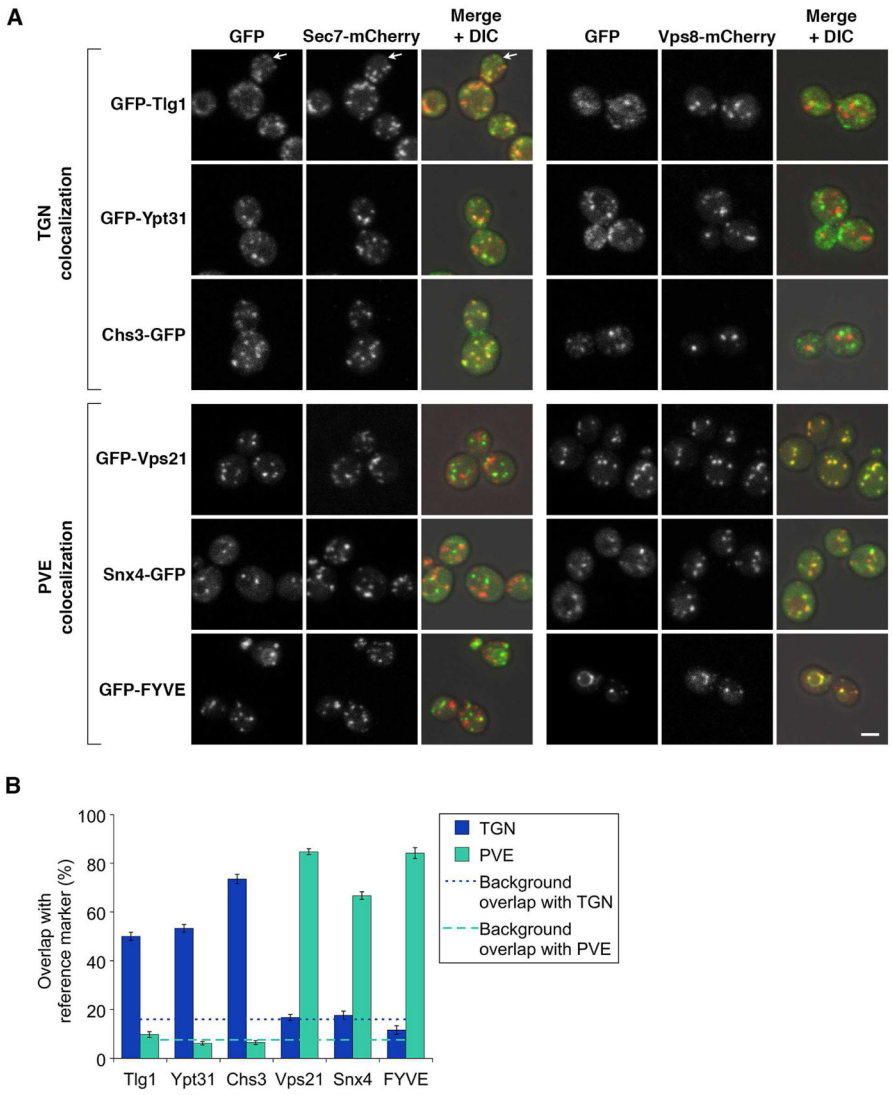

Figure 1. Candidate Yeast Endosomal Markers Localize to the TGN or PVE

(A) Colocalization analysis of candidate markers. Proteins were tagged with GFP and compared to reference markers by projection of confocal image stacks. Sec7-mCherry and Vps8-mCherry marked the TGN and PVE, respectively. Representative images are shown. Arrows indicate an example of Tlg1-labeled structures that did not label with the TGN reference marker. Scale bar is 2 μm.

(B) Quantification of the colocalization data. Colocalization for each pair in (A) was measured as the percentage of the GFP signal that overlapped with a mask created from the mCherry signal (Levi et al., 2010; Papanikou et al., 2015). Average colocalization was calculated using at least 48 cells per strain. Error bars indicate SEM. Background colocalization values for the TGN and PVE, taken from Papanikou et al. (2015), were calculated as the percentage of each reference marker signal that overlapped by chance with the other reference marker.

See also Figure S1.

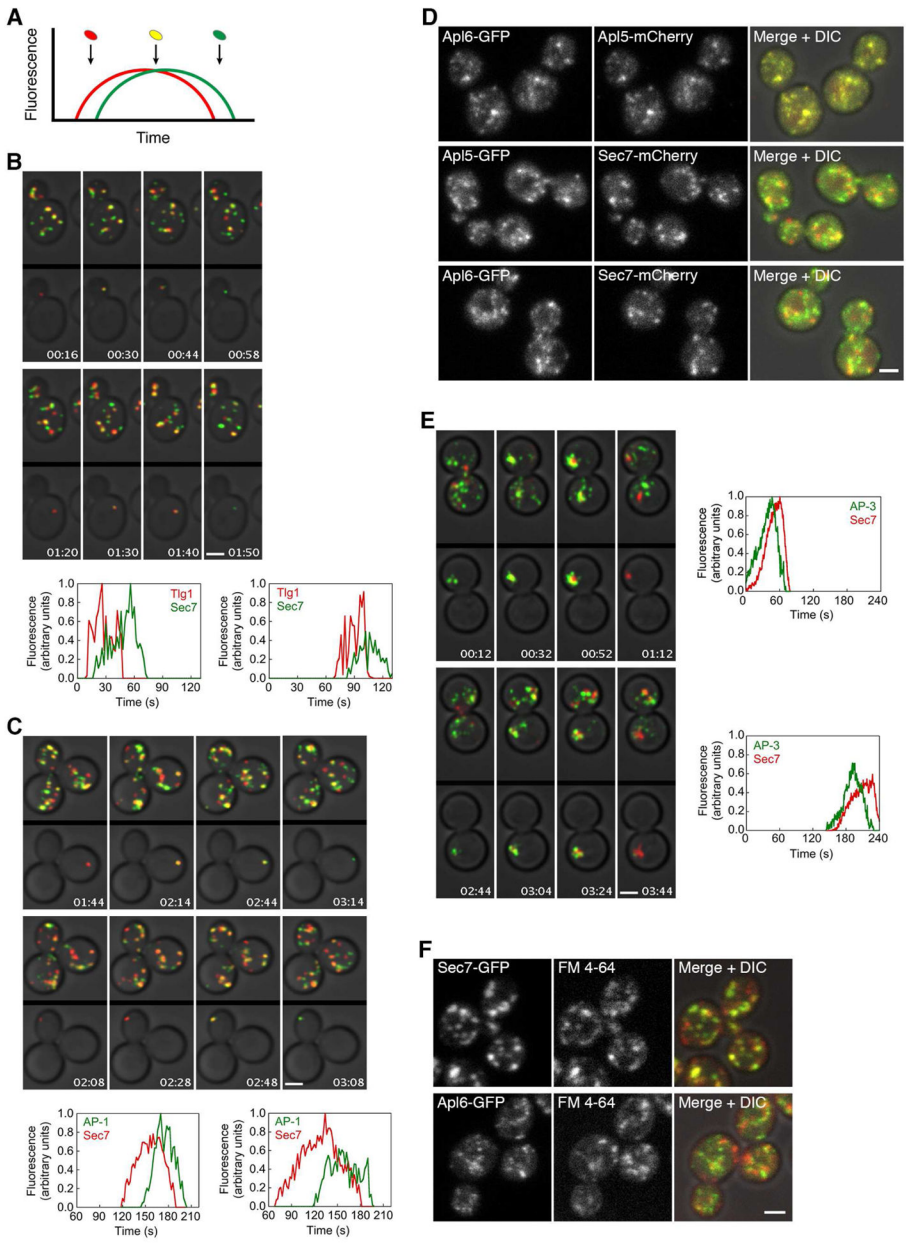

Figure 2. TGN Markers Label Maturing Compartments

(A) Simulated fluorescence traces for two temporally offset markers of a maturing Golgi compartment. The red marker arrives and departs before the green marker. Depending on the time when a static image is captured, the compartment may appear red, or yellow (red plus green), or only green.

(B) Kinetic tracking of the SNARE Tlg1, which marks the TGN but arrives and departs before Sec7. Cells expressing Sec7-GFP and HaloTag-Tlg1 labeled with JF_{646} ligand were imaged by 4D confocal microscopy for 5 min, and the image stacks were average projected. Representative frames from Movie S1A are shown. In the top half of each frame, the entire projection is visible. In the bottom half, the images were edited to show only a single TGN compartment. Two representative TGN compartments were analyzed. The plots show the

time-dependent fluorescence intensities for those two TGN compartments. Scale bar is 2 μm.

(C) Kinetic tracking of the AP-1 adaptor, which marks the TGN but arrives and departs after Sec7. Cells expressing Sec7-mCherry and the GFP-tagged Apl2 subunit of AP-1 were imaged and analyzed as in (B). Representative frames from Movie S1B are shown. Scale bar is 2 μm.

(D) Localization of AP-3 subunits. The Apl5 and Apl6 subunits of AP-3 colocalize perfectly with each other, but colocalize only partially with the TGN reference marker Sec7. Confocal image stacks were average projected. Scale bar is 2 μm.

(E) Kinetic tracking of the AP-3 adaptor. AP-3 is associated with the TGN but has a spatiotemporal pattern distinct from that of Sec7. *arf1*Δ mutant cells expressing Sec7-mCherry and Apl5-GFP were imaged and analyzed as in (B). Representative frames from Movie S3B are shown. Scale bar is 2 μm.

(F) Poor labeling of AP-3 structures with internalized FM 4-64. Cells expressing Sec7-GFP or Apl6-GFP were incubated with FM 4-64 at 22°C for 30 s, and then external FM 4-64 was quenched with SCAS and the dye was chased for 4 min to label the TGN. Confocal image stacks were average projected. Scale bar is 2 μm.

See also Movie S1, Movie S2, and Movie S3.

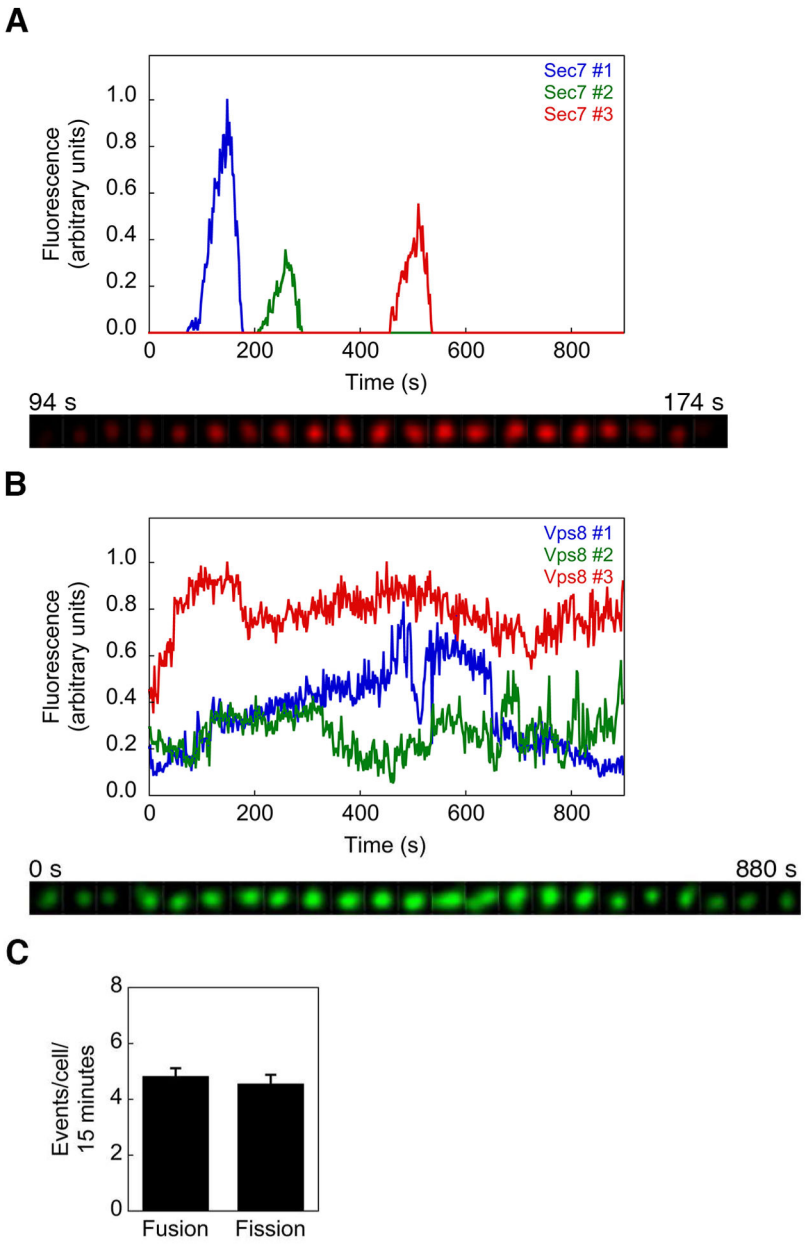

Figure 3. The PVE Is a Persistent Compartment

(A) Fluorescence traces for three representative TGN compartments labeled with Sec7-mCherry. In Movie S4, cells expressing Sec7-mCherry and Vps8-GFP were imaged by 4D confocal microscopy for 15 min. Three TGN compartments labeled with Sec7-mCherry were tracked for as long as the fluorescence signals were visible. Shown are average projected images of Sec7 structure #1 at 4 s intervals.

(B) Fluorescence traces for three representative PVE compartments labeled with Vps8-GFP. Those compartments were tracked for the duration of Movie S4. Shown are average-projected images of Vps8 structure #1 at 40 s intervals.

(C) Fission and fusion of PVE structures. For cells expressing Vps8-GFP, five 15-min 4D confocal movies were analyzed to count the number of PVE fission and homotypic fusion events. Bars indicate the average number of events per cell with SEM.
See also Movie S4 and Movie S5.

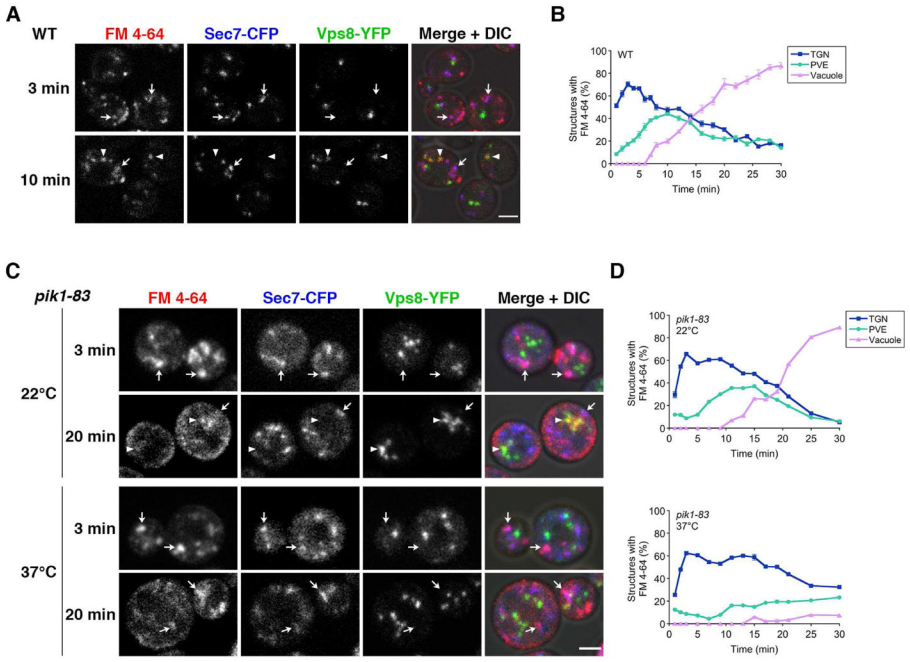

Figure 4. The TGN Is an Early Destination for Internalized FM 4-64

(A) Labeling of endocytic compartments with internalized FM 4-64. Wild-type ("WT") cells expressing Sec7-CFP and Vps8-YFP were incubated at 22°C with FM 4-64 for 30 s followed by SCAS. Confocal image stacks were collected at intervals up to 30 min after FM 4-64 addition. Representative average projections are shown for the 3 min and 10 min time points. Arrows indicate colocalization between Sec7-CFP and FM 4-64, and arrowheads indicate colocalization between Vps8-YFP and FM 4-64. Scale bar is 2 μm.

(B) Quantification of the data from (A). Localization of FM 4-64 in wild-type cells was quantified as the percentage of Sec7-labeled TGN structures, Vps8-labeled PVE structures, and vacuolar structures that showed detectable FM 4-64 signal. Mean ± SEM is shown for at least 32 cells for each time point.

(C) Labeling of endocytic compartments with internalized FM 4-64 in a *pik1* mutant strain. *pik1-83* cells expressing Sec7-CFP and Vps8-YFP were grown at 22°C, then half of the culture was shifted to 37°C for 15 min. Both halves of the culture were incubated with FM 4-64 for 30 s followed by SCAS. Confocal image stacks were collected at intervals up to 30 min after FM 4-64 addition. Representative average projections are shown for the 3 min and 20 min time points. Arrows and arrowheads indicate colocalization as in (A). Scale bar is 2 μm.

(D) Quantification of the data from (C). The analysis was performed as in (B) except that widefield images were examined. Mean ± SEM is shown for at least 35 cells for each time point.

See also Figure S2.

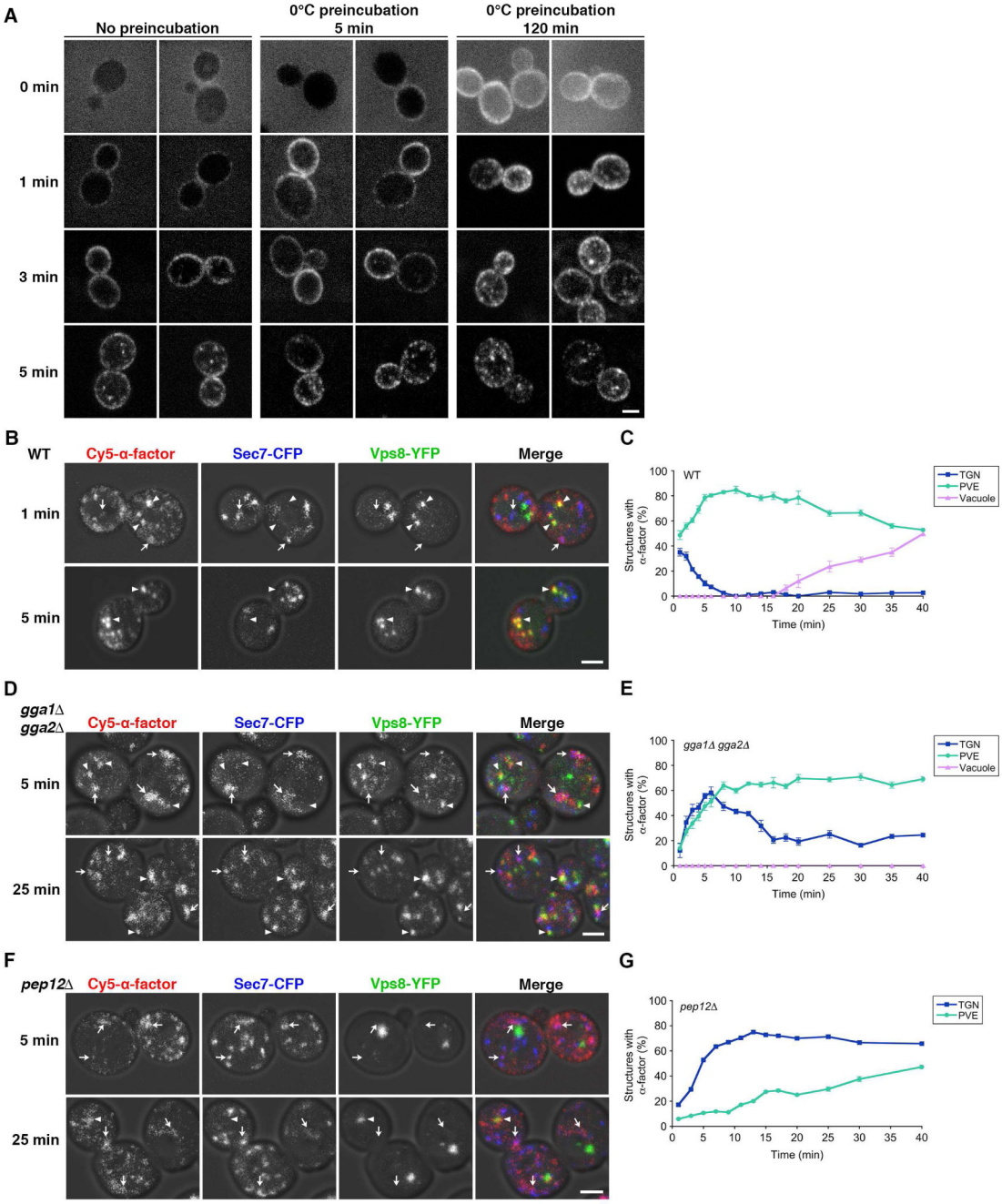

Figure 5. The TGN Is an Early Destination for Internalized α-Factor

(A) Internalization of Cy5-conjugated β-factor under different incubation conditions. Cells were either incubated with β-factor at 22°C and then fixed, or preincubated wit h β-factor on ice for 5 min or 2 h and then transferred to 22°C and fixed. Two representative average projections of confocal image stacks are shown for time points of 0, 1, 3, and 5 min at 22°C. With the concentrati on of labeled β-factor used here, saturation of β-factor receptors at the cell surface should have been almost immediate (Bajaj et al., 2004), so the faster

internalization seen after 2 h on ice was presumably due to accumulation of an endocytic vesicle intermediate. Scale bar is 2 μm.

(B) Labeling of endocytic compartments with internalized β-factor. Cells expressing Sec7-CFP and Vps8-YFP were incubated with Cy5-conjugated β-factor for 2 h on ice, then transferred to 22°C media and fixed at interva ls from 1 to 40 min after the temperature shift. Confocal image stacks were captured. Representative average projections are shown for the 1 min and 5 min time points. Arrows indicate colocalization between Sec7-CFP and fluorescent β-factor, and arrowheads indicate colocalization between Vps8-YFP and fluorescent β-factor. Scale bar is 2 μm.

(C) Quantification of the data from (B). Localization of β-factor was quantified as the percentage of Sec7-labeled TGN structures, Vps8-labeled PVE structures, and vacuolar structures that showed detectable fluorescent β-factor signal. Mean ± SEM is shown for at least 20 cells for each time point.

(D) Labeling of endocytic compartments with internalized α-factor in a *gga1*Δ *gga2*Δ mutant strain. *gga1*Δ *gga2*Δ cells expressing Sec7-CFP and Vps8-YFP were incubated with fluorescent α-factor and imaged as in (B). Representative average projections are shown for the 5 and 25 min time points. Arrows and arrowheads indicate colocalization as in (B). Scale bar is 2 μm.

(E) Quantification of the data from (D). The analysis was performed as in (C). Mean ± SEM is shown for at least 20 cells for each time point.

(F) Labeling of endocytic compartments with internalized α-factor in a *pep12*Δ mutant strain. *pep12*Δ cells expressing Sec7-CFP and Vps8-YFP were incubated with fluorescent α-factor and imaged as in (B). Representative average projections are shown for the 5 and 25 min time points. Arrows and arrowheads indicate colocalization as in (B). Scale bar is 2 μm.

(G) Quantification of the data from (F). The analysis was performed as in (C), except that no vacuolar localization was detected. Mean ± SEM is shown for at least 90 cells for each time point.

See also Figure S3.

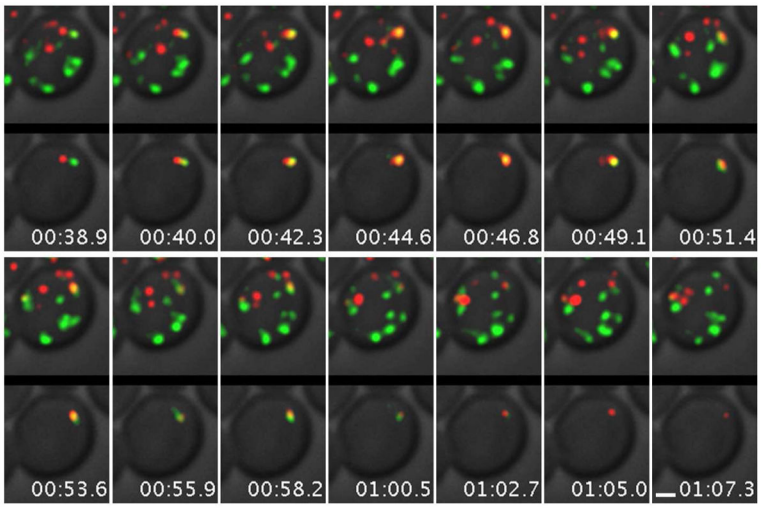

Figure 6. Yeast Endocytic Vesicles Fuse with the TGN

A 5 s pulse of FM 4-64 followed by SCAS were applied in a flow chamber to cells expressing Kex2-GFP. The cells were then imaged by 4D confocal microscopy, and the image stacks were average projected. Selected frames show a cell from Movie S7A, either unedited in the upper panels, or edited in the lower panels to focus on a single endocytic vesicle merging with a TGN compartment. Time is calculated from the start of the FM 4-64 pulse. Scale bar is 1 μm.

See also Figure S4, Movie S6, and Movie S7.

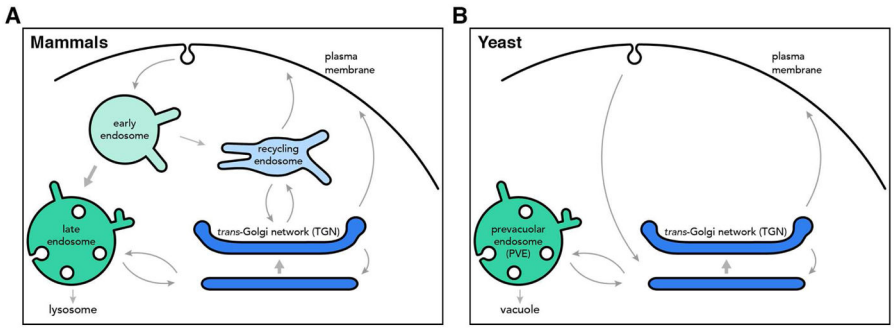

Figure 7. Comparison of the Mammalian and Yeast Endocytic Pathways

(A) In mammalian cells, endocytic material is delivered to early endosomes, which mature into late endosomes that subsequently fuse with lysosomes. Early endosomes also send material to recycling endosomes for return to the cell surface. Recycling endosomes are related to the TGN with regard to localization and membrane traffic machinery. Late and recycling endosomes communicate with the TGN through bidirectional traffic.

(B) In yeast, endocytic material is delivered to maturing TGN compartments. Internalized material is then either recycled to the cell surface, or delivered to stable PVE compartments that are postulated to undergo “kiss-and-run” events with the vacuole. Some components recycle from the PVE to the TGN. The yeast TGN can be viewed as combining properties of the mammalian TGN and recycling endosomes, and the yeast PVE can be viewed as combining properties of the mammalian early and late endosomes.